MISSOURI
S&T
Library and
Learning Resources

Scholars' Mine

Masters Theses

Student Theses and Dissertations

1971

An investigation of a bistable oscillator used in a phase modulated control circuit

Yu-Fang Yen

Follow this and additional works at: https://scholarsmine.mst.edu/masters_theses

Part of the Mechanical Engineering Commons

Department:

Recommended Citation

Yen, Yu-Fang, "An investigation of a bistable oscillator used in a phase modulated control circuit" (1971). *Masters Theses*. 7234.
https://scholarsmine.mst.edu/masters_theses/7234

AN INVESTIGATION OF A BISTABLE OSCILLATOR USED
IN A PHASE MODULATED CONTROL CIRCUIT

by

YU FANG YEN, 1942-

_____

A

THESIS

presented to the faculty of the graduate school of

UNIVERSITY OF MISSOURI - ROLLA

in partial fulfillment of the requirements for

the degree of

MASTER OF SCIENCE IN MECHANICAL ENGINEERING

Rolla, Missouri

1971

_____

Approved by

_____ (Advisor)   _____
_____

ABSTRACT

A primary component in the investigation of phase modulated control systems is bistable oscillator which converts a constant oscillation signal to control the system. The oscillator is feedback type that utilizes a feedback capacitance and resistance in each feedback path to change its frequency. The theoretical behavior of bistable oscillator was investigated and the non-dimensional results were set for convenience in determining the oscillation period.

The control circuit which based on the oscillator was also presented a form of suitable circuit for direct application to practical control problems.

ACKNOWLEDGEMENTS

The author would like to express his appreciation to Dr. Donald A. Gyorog for his help and guidance in writing this paper and for the many favors he performed while the author was a non-resident student.

The author is also thankful to Mrs. Connie Hendrix for her cooperation in typing this thesis.

TABLE OF CONTENTS

TABLE OF CONTENTS (continued)

LIST OF ILLUSTRATIONS

LIST OF ILLUSTRATIONS (continued)

LIST OF TABLES

LIST OF SYMBOLS

b_o	width of nozzle
R	radius of jet
α	side wall angle
θ	attached angle
X	distance of reattached point
$\overline{X}$	length of main jet at any point
L	offset $+ \dfrac{b_o}{2}$
u	velocity of local point
V	bubble volume
U	velocity of jet at jet centerline
E	overall jet entrainment rate
Q	volume flow per unit depth in main jet
Q_s	main flow in main jet exit
Q_c	volume flow in control line
$C_{\Delta P}$	$C_{\Delta P} = \dfrac{P_b - P_\infty}{\frac{1}{2}\rho u_o{}^2} = \dfrac{-P_{bg}}{P_{jg}}$
$V*$	non-dimension bubble volume
Q_1	volume flow to the feedback path
V_f	volume of feedback capacitance
C_f	feedback capacitance $\dfrac{in^5}{lb\text{-sec}}$
P_{fa}	average pressure in feedback capacitance
C_c	bubble capacitance

R_c — resistance of control port

R_f — feedback resistance $\dfrac{lb\text{-}sec}{in^5}$

P_o — working output pressure of amplifier

τ_f — time constant $\tau_f = R_f C_f$

τ_c — time constant $\tau_c = R_c C_c$

ω_n — natural frequency of oscillator

ξ — damping ratio

R_L — load resistance

R_o — output resistance

C_o — output capacitance

P_s — supply pressure $P_s = P_{jg}$

t_{os} — oscillation period

f_{os} — oscillation frequency

P_c — control port pressure $P_c = P_{bg}$

I. INTRODUCTION

In 1932 Henri Coanda (1) described the characteristics of wall attachments, and observed that as a free jet emerges from a jet nozzle the stream will tend to follow a near-curve on an inclined surface and will even "attach" itself to or come into contact with and flow along this surface if the curvature and inclination is not too large. In 1938 A. Metral and K.P. McMahan (2) contributed to the understanding and use of this effect by demonstrating that fluid flow could be controlled by utilizing the aerodynamic flow properties of a fluid jet. In 1940, the jet-on-jet control of the power stream was invented and the modern fluidic elements were formed.

In 1958, the work which Moore and Kline (3) did in the United States demonstrated that a jet could have two or three stable states. This indicated that no-moving-part-devices have a potential logic capability. Based on this, the bistable amplifiers and logic systems were built. The fluidic logic system is closely analogous to the electronic system in function. The major difference between the two technologies lies in the speed of operation. The electronic system switches near the speed of light, while the fluidic system switches near the speed of sound. In a machine tool control system, the fluidic logic controller which switches faster than the equivalent electro-mechanical control, can allow shorter machine cycle times.

As a result of the reliability and many advantages of automation, the development of suitable fluidic-logic systems has been undertaken; the behavior of the controller, and the selection of the power source of the actuator are important to the analysis of the system. During the past few years it has become evident that the theoretical point of view dealing with the connection between the valve actuator and amplifier is more difficult to analyze than that of the electro-valve control system. The direct control of hydraulic or pneumatic actuators by the output of the fluidic circuit eliminates the need of the solenoid valves required by electrical system. In addition, the fluidic-logic system is usually simpler and easier to maintain than the other logic systems.

Further development of fluidic-logic systems in attempting to overcome the deficiencies of the then existing energy systems was done by R.E. Bowles, W.M. Horton and R.W. Warren at Harry Diamond Laboratories (4) in Washington in 1959. They used a fluidic logic system which can develop higher speeds than pneumatic and hydraulic systems which operate in the same environments with lower speeds. Since 1963, the question of an "ideal" fluidic-logic system for industrial applications and also for the 'mild' environmental military requirements has been under study at the Aviation Electric Company (5). In 1963, the theoretical and practical logic systems were undertaken,

and there are many proved systems already widely used in
the industrial cutting machine and press process operations.
An automatic checking and grading device for geometric
dimensional devices was designed with a sequential-control
fluidic-logic circuit by M. Monge (6) in 1967. In the same
year the numerical positioning in machine tools by means of
fluidic-logic systems was investigated by H.P. Stal, I.
Bulk. The fluid-logic systems have demonstrated the advan-
tage of reliability, ease of maintenance and economy over
other control systems.

Practical applications of multiple step wise position
control processes by means of fluidic-logic-hydraulic
systems in handling work processes was explored by D.
Bouteille (8). A schematic of his control systems is
shown in Fig. 1. This is one of the better illustrations
of the application of multiple position controls with
fluidic-logic elements in industrial operation. In this
system, the author used bistable amplifiers to directly
operate servo-valve M to achieve the position control
process. Since the bistable amplifiers are usually
influenced by the output loading, the change of the loading
from the servo-valves could cause the variation of output
of the bistable amplifier. Another effect which influences
the positioning accuracy is the initial momentum of
actuator motion. If these problems can be solved and a
better circuit can be formed, the completed system for

position control would be extremely useful for precise machine tool position and other similar applications.

The position control system shown in Fig. 1 operates in the following manner. When the part to be positioned contacts the valve f, the servo-valve Mo is operated by the flow through valves 'f', 'a', 'b' and 'c'. The actuator M then positions the part at position 'C' and then retracts. The next part to be positioned contacts the valve 'f' and then will be pushed to position 'B' by actuator M acted by servo-valve Mo under the action of valves 'a' and 'b' only. When this part reaches position 'B', the actuator retracts and in like manner a third part will be pushed to position A by actuator M operated by servo-valve M under the action of valve 'a' only. The parts which have been positioned at points A, B, and C then cause the valve 'd' to open. The actuator L acted upon by the flow through valve 'd' moves the parts forward to the roller bed. In the meantime the valve 'e' is open. The flow which passes through valve 'e', then to 'g', causes the actuator L to retract and then the cycle of operation repeats.

In an attempt to reduce the inaccuracy of position control operation, an improved control circuit is presented in this report, it is shown in Fig. 2-1. This control cir-cuit consists of a bistable oscillator and four-input bistable amplifier which were connected to the multi-position
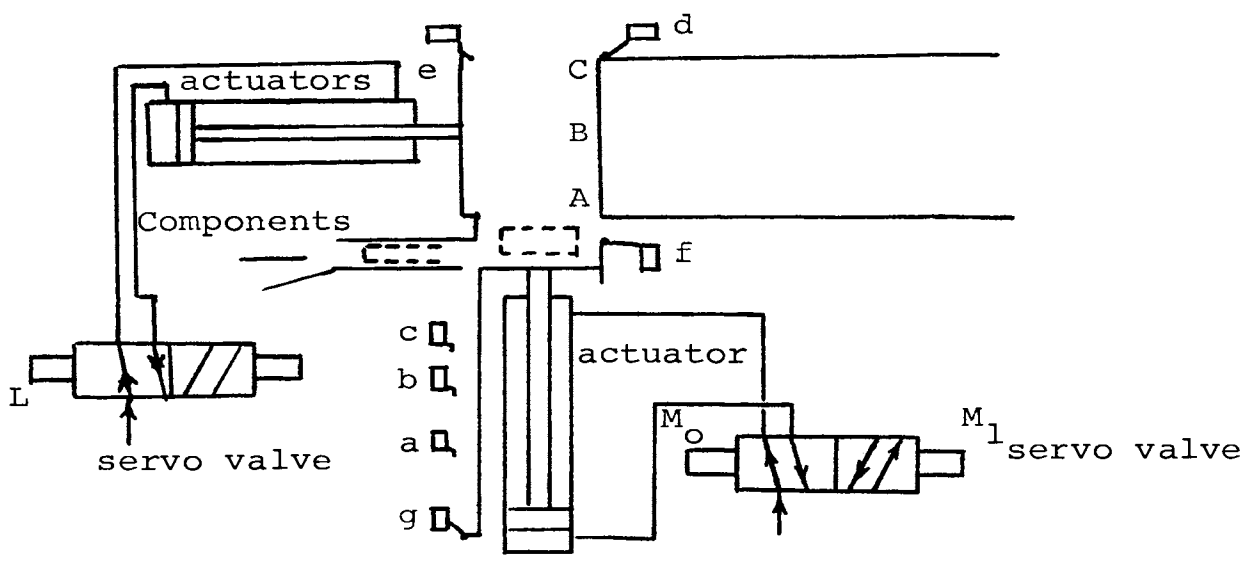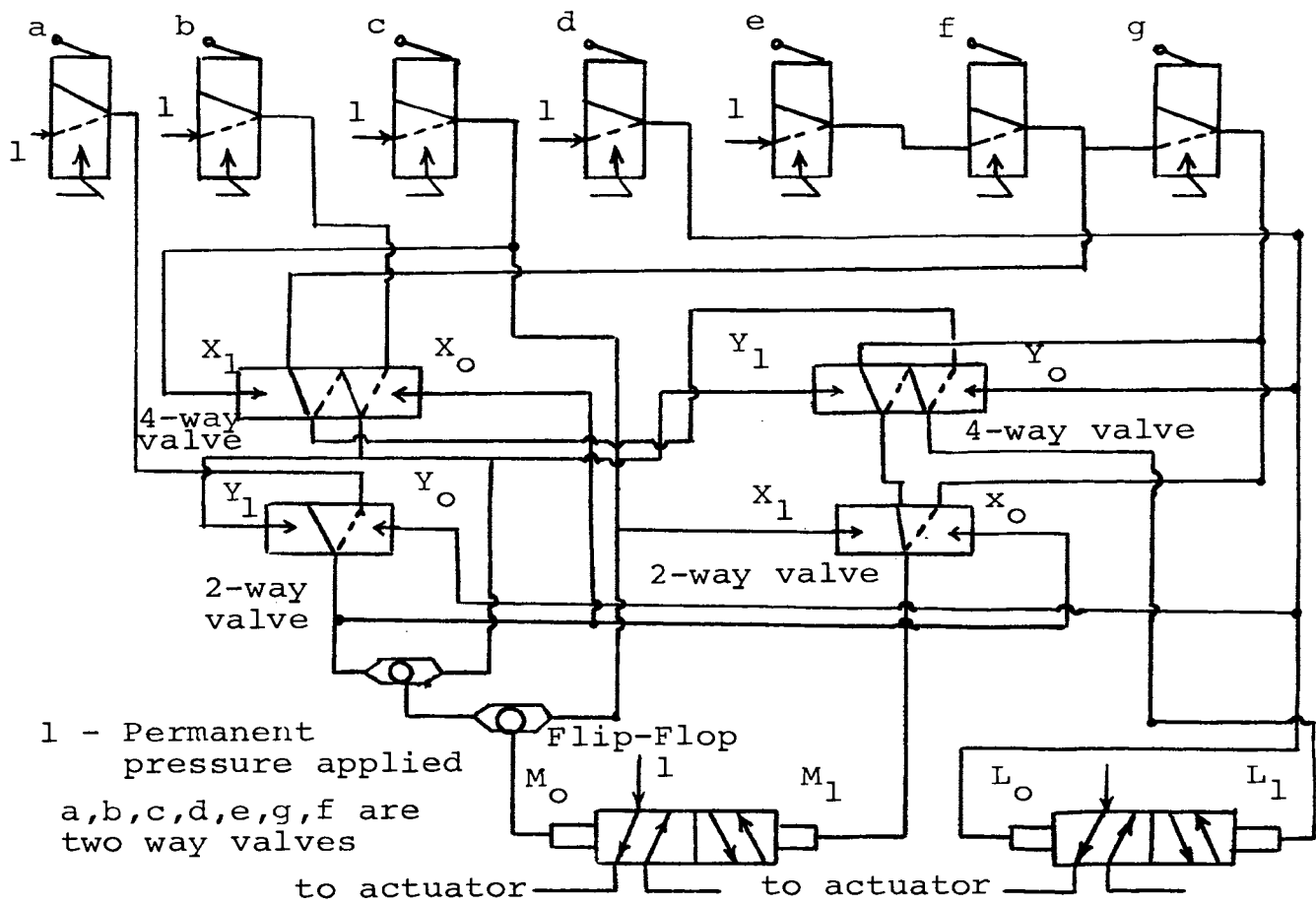
Figure 1. Handling work process system

actuator. It was decided to use the constant oscillating signal from the bistable oscillator to operate with error signal (ΔP) to control the position system. The range of operation frequency becomes important to the characteristics of the multi-position actuator operation. In case of high frequency operation when $\Delta P = 0$ the output of sample device does not have enough flow to open the servo valve and therefore operate the actuator. At very low frequencies, the accuracy of the control is reduced because of the large amplitude oscillations of the control signal. Thus the characteristics of the oscillator and a control circuit were investigated and the purpose of this thesis was to formulate design and analysis techniques for the bistable oscillator in the control circuit in conjunction with a hydraulic multi-position actuator.

II. DESCRIPTION OF CONTROL SYSTEM CIRCUIT

The control circuit shown in Fig. 2-1 consists of a bistable oscillator, a four input bistable amplifier and a power bistable amplifier whose outputs are connected with the hydraulic servo actuator.

The bistable oscillator which provides the oscillating signal and drives a sampling pulse device was selected for these reasons:

(1) From a comparison of the output wave forms of proportional oscillator (18), the bistable oscillator produced a more symmetric output and a more even on-off time between the two outputs.

(2) The bistable devices had an advantage that the output flow could be adjusted more easily than the proportional amplifier by variation in supply pressure.

The period of the oscillating wave will be a function of the time required for the output signal to traverse the feedback path and the transport time of the stream between the nozzle and the output receiver. Although the transport time of the amplifier does not vary with frequency, it is extremely sensitive to the attenuation of the feedback signal.

bistable   time delay   four input   sample pulse
oscillator (signal modu-   bistable   device
           lation)   amplifier

P_f

P_{in}

x_i
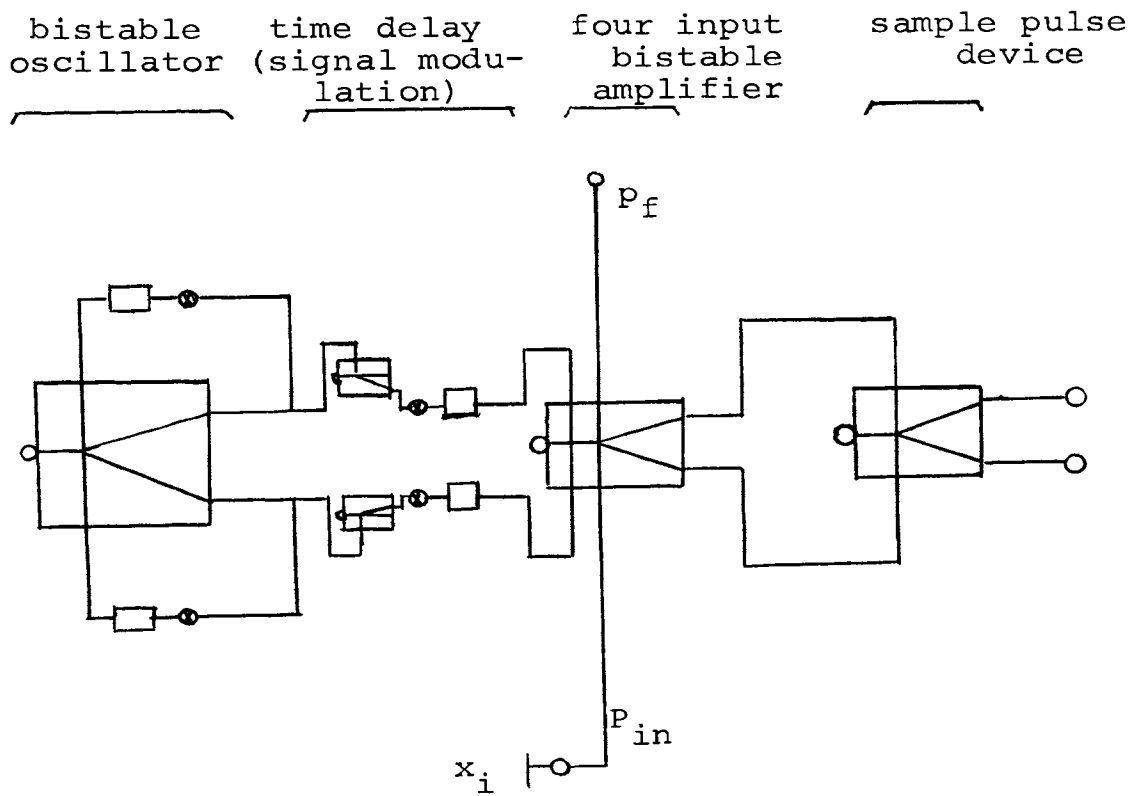
Figure 2-1.   control circuit

Since the frequency of oscillation depends on the capacitance and resistance of the feedback path, with a suitable capacitance for delay or resistance for attenuation in the feedback path of the oscillator one can design a particular frequency for driving the sample pulse device. For further improvement of preventing the output loading effect on the oscillator element, the output can be used to drive an 'or' amplifier.

R.C. Modulation Circuit:

The smooth "sinusoidal" type of pressure oscillation is then obtained by a resistance and capacitance combination ahead of the four-input bistable amplifier. The output of the oscillator is "square pulse" oscillation rather than a sinusoidal oscillation, so with this R.C. smoothing the oscillating input at the four input bistable amplifier has the advantage of improving the sensitivity and modulation of the output pulse width with error signal (Δp).

Four - Input Bistable Amplifier:

Following the R.C. circuit is the four input bistable amplifier. This device has two sets of control ports. One set of control ports is connected to the R.C. circuit modulated oscillator output. The other set is used for the proportional pressure error signal (Δp) emitted from the position pressure sensor. It is important to note that both sets of controls must be located in the
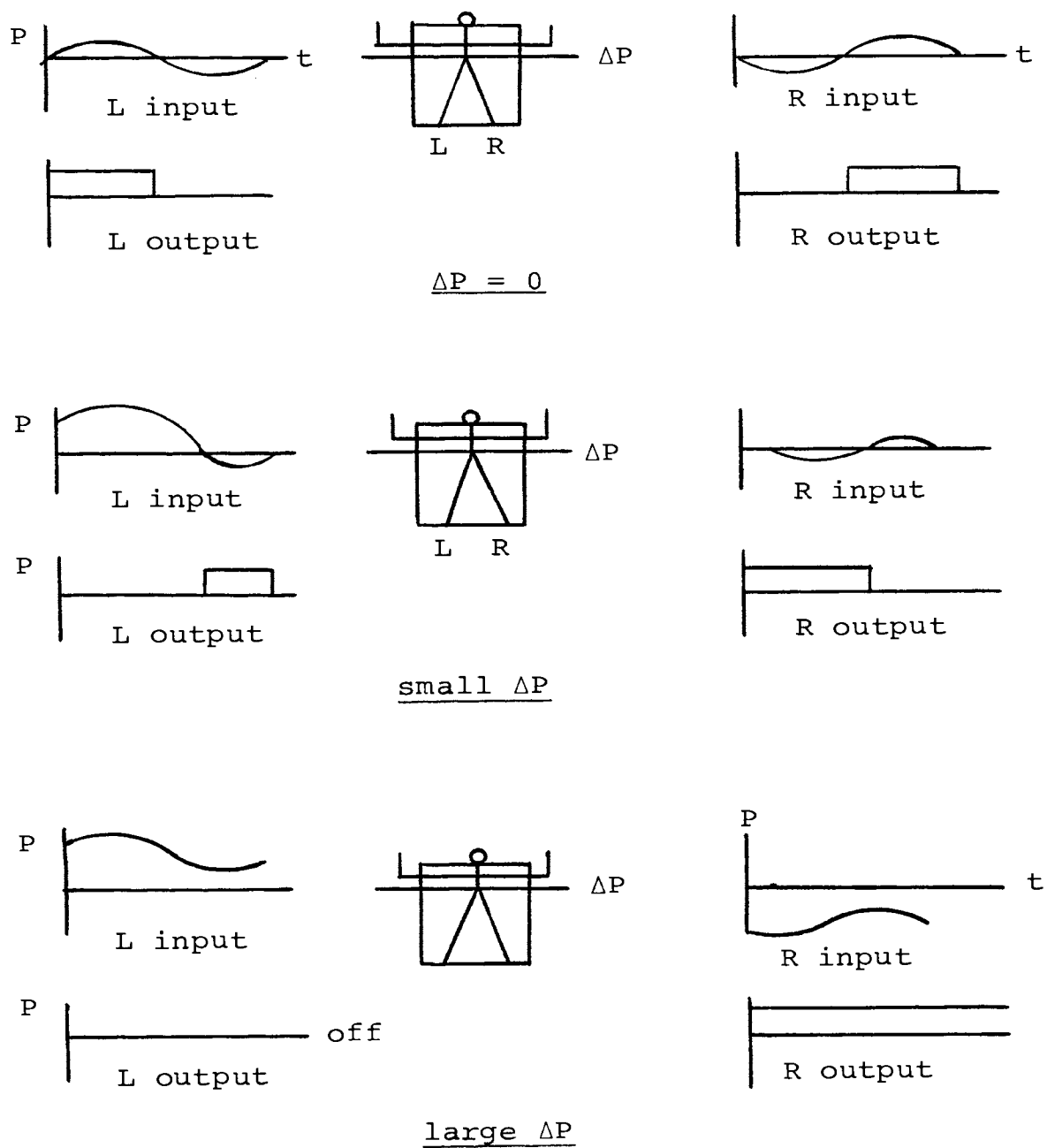
Figure 2-2. Illustration of ΔP input on output pulse modulation (a. $\Delta P = 0$, b. small ΔP, c. large ΔP)

entrainment bubble of the power jet. If the error signal input is located in the attachment region of the power jet, a very large signal from the sensor would be required to switch the power jet. In operation, the bistable oscillator produces an oscillating signal; then if signals of equal magnitude are applied to the error signal inputs (ΔP) of the four input bistable amplifiers, the flow out of this amplifier is balanced. That is, the output flow issues from each output port for the same length of time. This behavior is illustrated in Fig. 2-2a. The application of a differential signal input, ΔP, to the secondary control ports of the four-input bistable amplifier produces a variable pulse width output as shown in Fig. 2-2b. If the error signal is very large, in this case the oscillator is still oscillating but it does not have enough momentum to overcome the input error signal, the output issues only from one side of the four-input bistable amplifier, i.e. The jet is held over on one side and all off on the other. This behavior is illustrated in Fig. 2-2c.

Power Amplifier:

The last stage of control circuit is the high flow gain and pressure gain bistable amplifier (Fig. 2-1). Using this device which applies the high supply pressure, the output pressure and flow quantity of the sample pulse

output is increased. This causes enough flow and high pressure to operate the servo-valve.

If the operation of the oscillator has no temperature effects, the system will oscillate at constant frequency. Using this control circuit in conjunction with a hydraulic of pneumatic actuator, the step wise or continuous position control system can be designed. Several circuits for connecting the variable output pulse with the actuator were considered. All of these were based on sensing and control circuit illustrated in Fig. 2-1.

Stepwise Position Control System:

This system circuit was shown in Fig. 2-3. The operation of this system was controlled by the on-off button valves L', and R'. When the button valve R' is on, the input pulse open to X amplifier and so the X_1 amplifier switches to '02' acting on the servo valve that causes the actuator to move downward until valve R' is released. When valve L' is on, the pulse opens forward to Y amplifier and so the Y_1 amplifier switches to '01' acting on the servo valve making the motion forward and stop at the pre-determined position S. From this circuit, several pre-determined stepwise position control systems can be designed.

button valve

input
pulse

L`   Y   bias

O1 O2

oscillator
signal
pulse

input
pulse

R`   X   bias

O1 O2

S

X₁

O1

O2

Loading
Amplifier

servo
valve
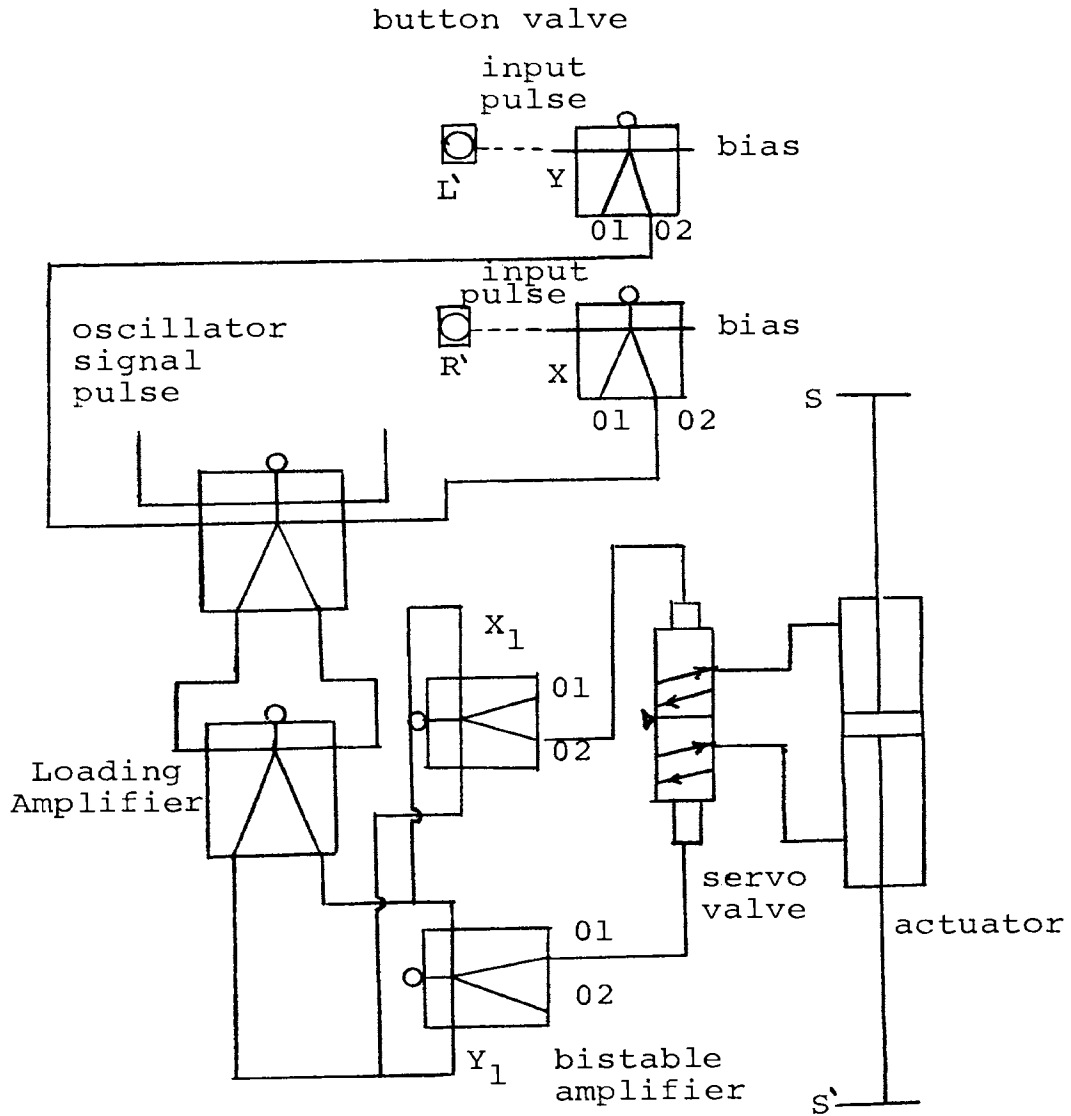
actuator

O1

O2

Y₁   bistable
amplifier

S`

Figure 2-3.   Stepwise position control
system

Continuous Position Control System:

The simplest system is shown in Fig. 2-4. In this system the output of the sample device is directly connected to the actuator. If the supply pressure of a bistable amplifier '1' and '2' was $P_{s2} > P_{s1}$ and the oscillating frequency is higher than the natural frequency of the actuator, then the slow motion - quick return system can be designed. The accuracy of this system depends on the phase modulation, thus high gain and large modulation is required for this system.

For greater force output the system as shown in Fig. 2-5 was used. The sample pulse amplifier is connected by the hydraulic servo actuator, therefore pneumatic-hydraulic control system was formed.

Based on the circuit shown in Fig. 2-1, the sampling signal and variable pulse circuit shown in Fig. 2-6 was conceived. With this circuit the more sophisticated continuous position control system can be built. The more sophisticated system employs sampling the variable output pulse with a fixed time-based sampling pulse. This system is shown in Fig. 2-7. At zero error pressure signal, the pulse does not overlap in time and therefore will not trigger an "and" unit, but with an error signal present the pulse from one output will overlap its respective sampling pulse and give an output signal to operate the actuator.
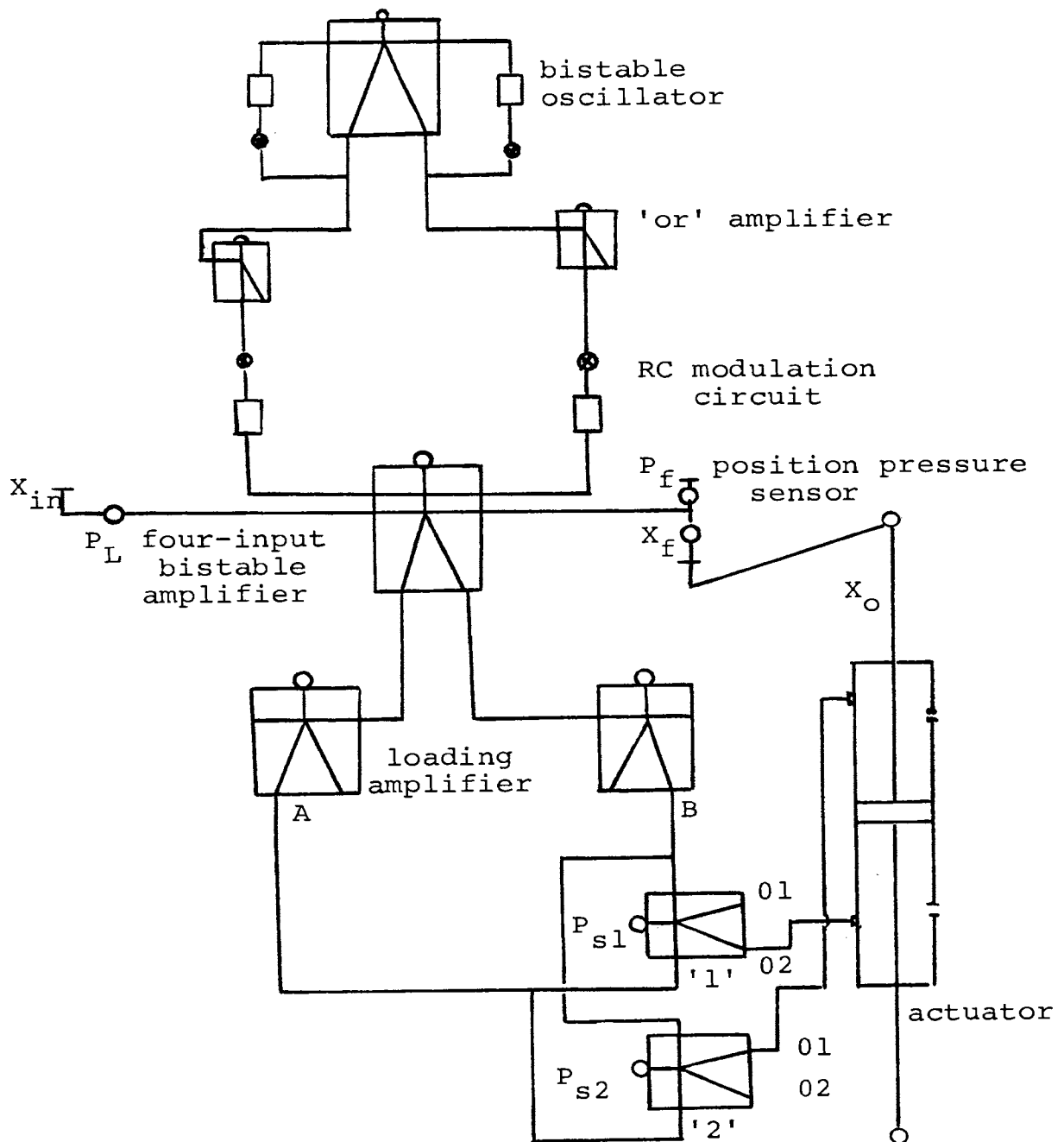
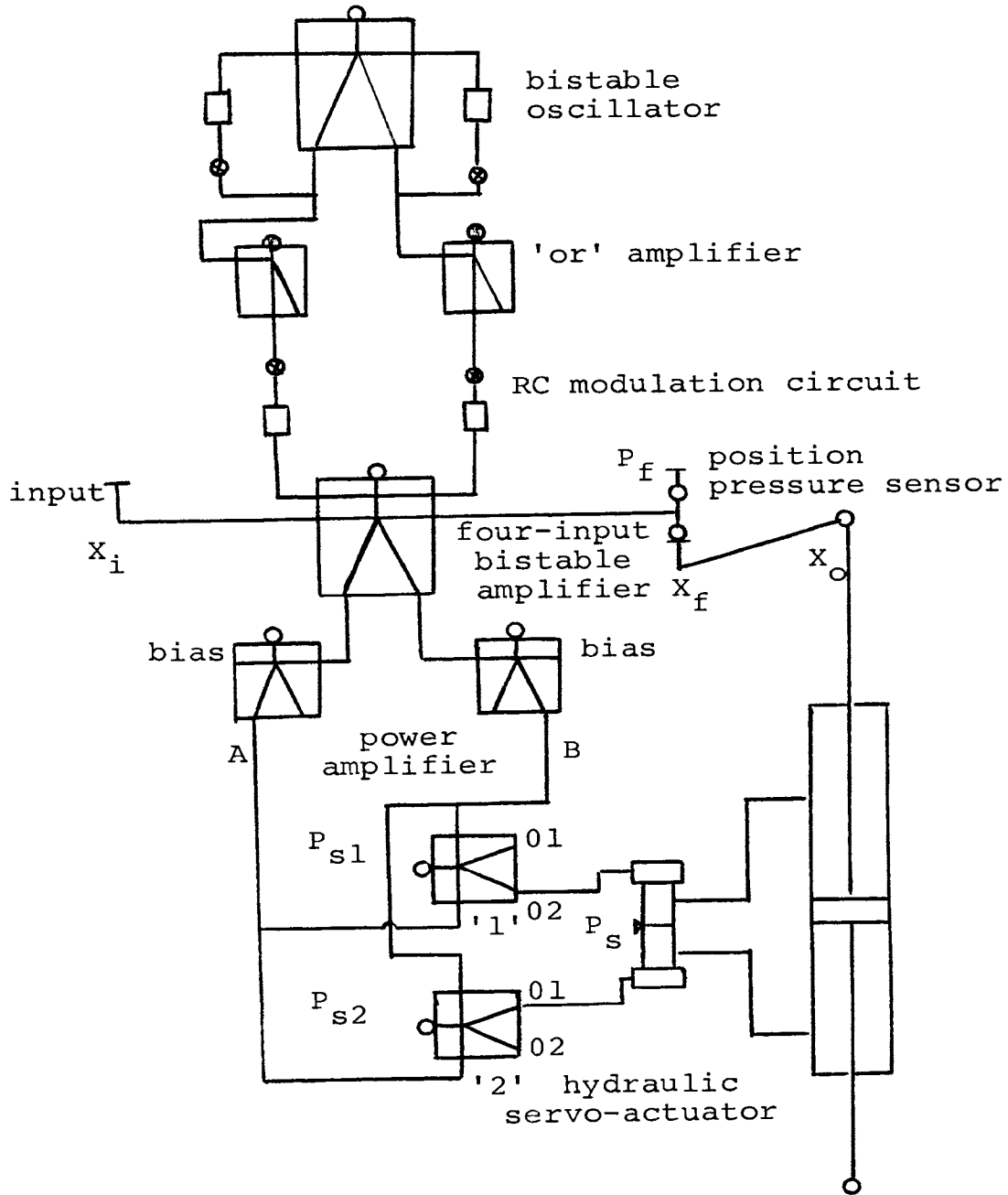Figure 2-4. Slow motion and quick return system

Figure 2-5. Pneumatic-hydraulic position control system

In locating the correcting phase relation between the variable output pulse and sampling pulse, the capacitance is adjusted until the sampling pulse occurs just after or just before the variable signal pulse with a zero error pressure signal. A slight modification for locating the signal and sampling pulses in time is shown in Fig. 2-8. For the positive Δp error signal the system drives the actuator in the positive direction. A pressure signal proportional to this motion is fed back to decrease the error pressure signal and stop the actuator at the desired position. For a negative ΔP error signal the system operates in reverse direction to the reference position and stops. Thus, continuous position control is achieved.

Typical applications of stepwise control system are the positioning process and the drilling process. By means of pushing a button valve, the predetermined position can simply and easily be controlled. Hence, highly skilled personnel are not essential. The operation of this system is limited to constant speed on-off operation, therefore the stepwise control system is not suitable for controlling such variables as fuel consumption or other multi-position quantities. These kinds of system can be controlled by means of sampling pulse modulation and continuous control. The ability to handle complex control systems by simple methods and provide a wide range of adjustment make the continuous control system more useful than stepwise control system.

1'

1

sampling   pulse

control error signal
ΔP

2'   2

variable pulse
output
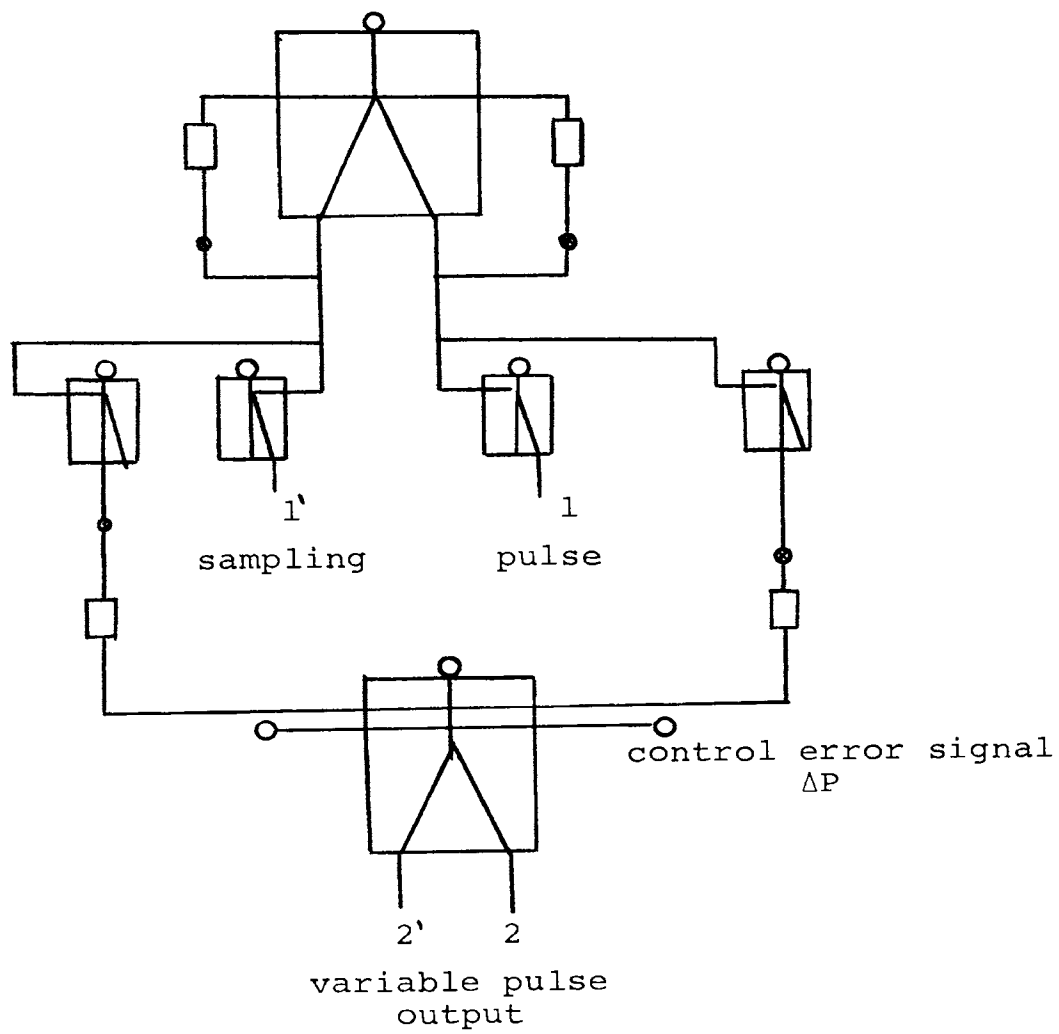
Figure 2-6.   Variable time pulse system
               circuit
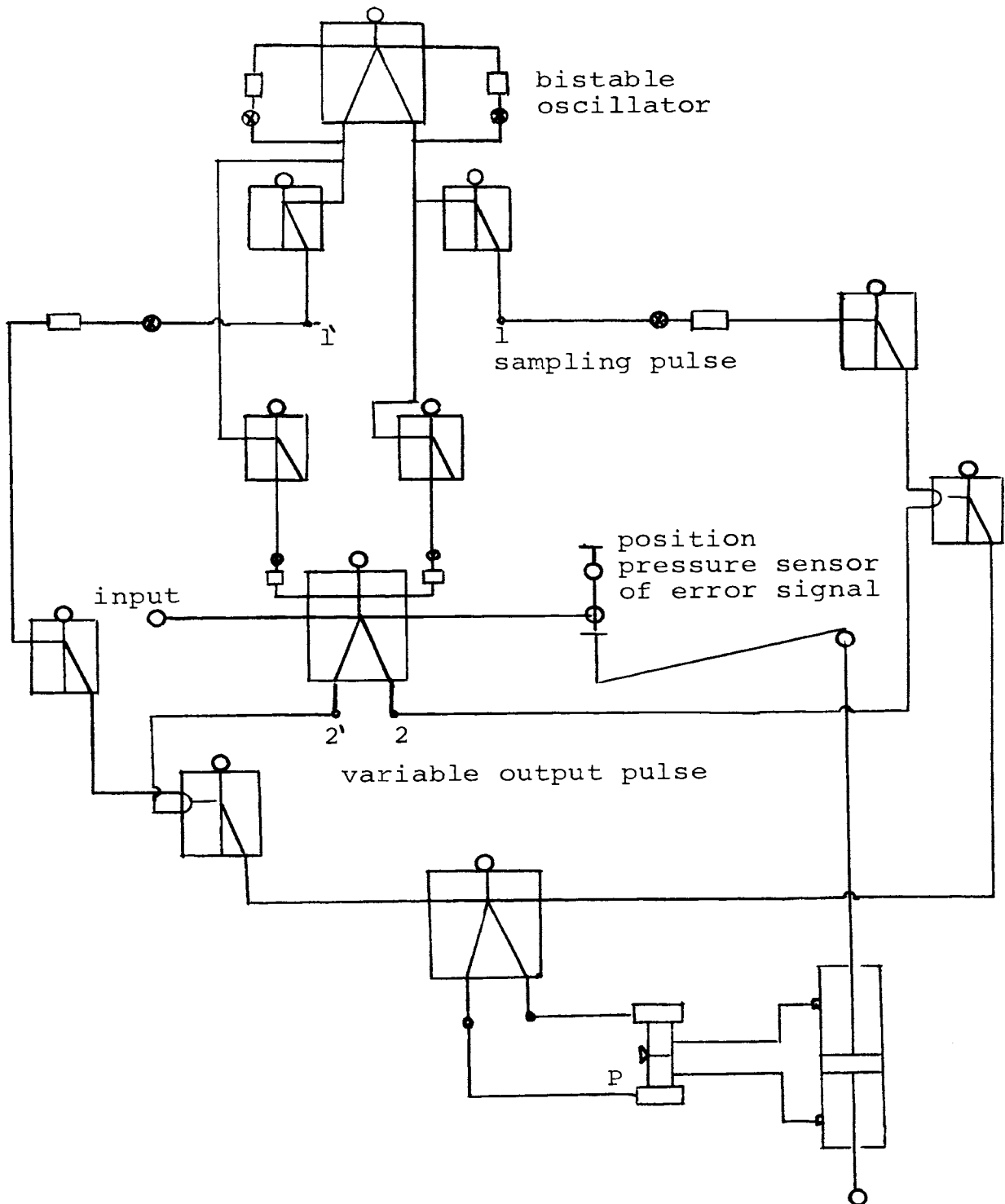
Figure 2-7.   Continuous position control system circuit

①.. sampling
     pulse from
     oscillator

②.. variable signal
     pulse from
     bistable
     amplifier
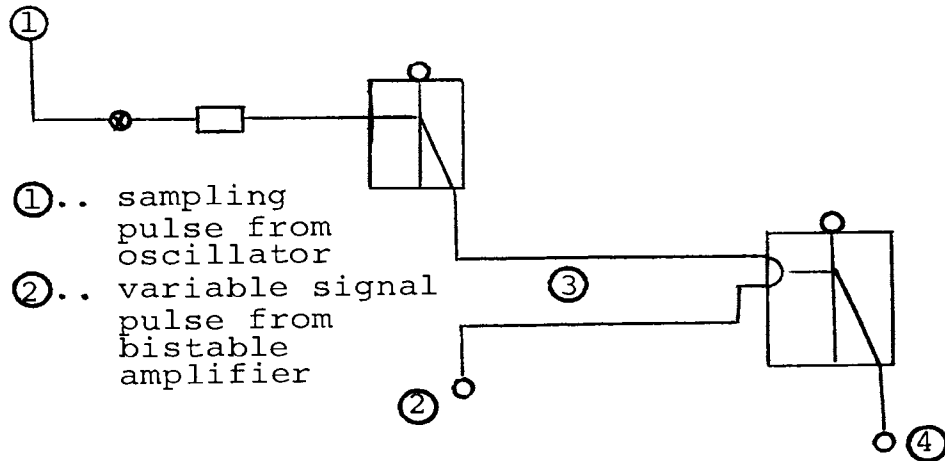
a. Variable time duration pneumatic
     pulse circuit

When zero error signal pressure $\Delta p = 0$
the pulse duration of ① and ② is the same so ④
is off.

④ ——————————————————— off

For larger positive error $\Delta p > 0$ (signal pulse all-on)

①

② ——————————————————— on ↑

③

④
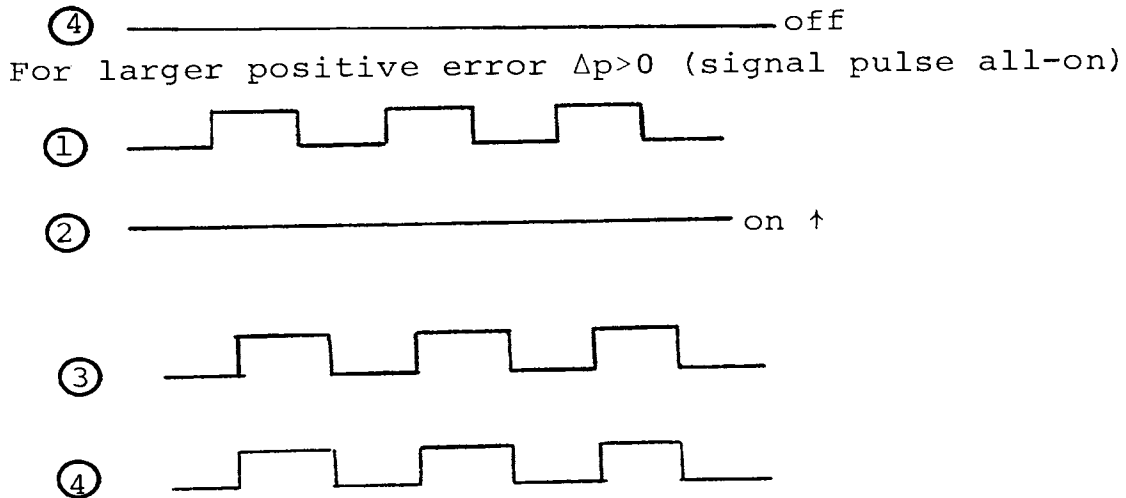
b. Pulse location

Figure 2-8. Variable time duration pneumatic
     pulse (a. variable time duration
     pneumatic pulse circuit, b. pulse
     location)

One of the basic elements of the control circuits described in this chapter is the oscillator. The mechanism of its operation is analyzed in the following chapter. The dynamics of the servo-valve and actuator have been detailed in reference (14), and for this reason it is excluded in this paper.

III. BISTABLE AMPLIFIER OSCILLATOR

The oscillation period is a function of the time for the flow to traverse through the feedback path to reach the required switching level and the transport time of the bistable amplifier. To calculate the oscillation period these time delays have to be described. The mechanism of the switching process itself is dependent on the type or geometric construction of the bistable amplifier. The major types are terminated wall or bleed type of switching, contacting-both wall type of switching, and splitter type of switching.

The wall attachment fluidic devices are digital output elements which utilize the Coanda effect. The operation of the bistable amplifier requires a supply or power stream, which is introduced through the power nozzle to convert a great deal of the stream's static pressure or potential energy into the power jet velocity head. Located at either side of this power nozzle are channels for control streams which can deflect the direction of the power jet. Deflection is accomplished in the digital output device when the entrainment properties of the jet are compensated, causing it to attach to one or the other side walls.

Hence, the wall attachment bistable fluid amplifier operates because of the entrainment characteristics of a submerged fluid stream. Shifting the stream from one wall to another is accomplished with the control stream. Notice the
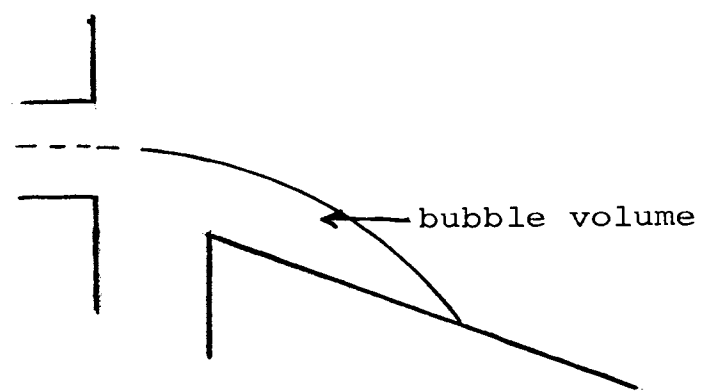
Figure 3-1. Illustrated bubble volume

'bubble' in Fig. 3-1 between the jet nozzle and the point of attachment to the wall. This is a low pressure vortex region which is sealed by the high pressure jet stream. The fluid is entrained from this region near the jet nozzle and is replenished by the jet itself near the point of attachment. The existance of the pressure differential between the outer edge of the jet and the low pressure region next to the wall maintains the jet attachment. If there are no changes, this equilibrium condition will allow the jet to flow along the wall continually. In order to change this condition it is necessary to increase the pressure within this bubble until it exceeds the pressure on the outer edge of the power jet. This is accomplished by injecting additional fluid through the control part and into the bubble. If the rate of fluid injected into the bubble exceeds the rate at which fluid is removed by entrainment, the pressure on the inner edge of the jet increases, and subsequently the jet will be forced to detach from one wall and attach to the opposite wall.

The switching process as noted previously can be classified into three basic types as follows:
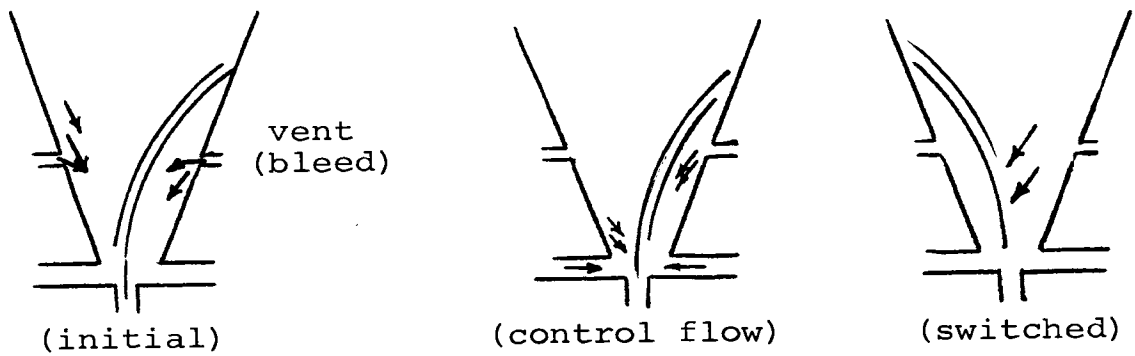
1. Terminated wall or bleed type of switching,

2. Contacting both wall type of switching,

3. Splitter type of switching.

These are illustrated in Fig. 3-2. The left hand view is the initial steady-state condition, the middle view

indicates the effect of adding control flow, and the right hand view indicates the completion of switching.

Terminated-wall or bleed switching

The terminated-wall or bleed type of switching is characterized by the separation bubble's communicating with the atmosphere prior to the power jet's contacting the opposite wall or the splitter. When the boundary walls are very short the amplifier does not behave in a bistable manner. The separation bubble can not form because the atmosphere has ready access to both sides of stream. In fact, with the side walls just short of the reattachment region the stream will oscillate between the two walls. As a consequence, stability is very low and the gain is very high, only a very small control signal is necessary to hold the stream on the wall. When the side walls are extended far enough downstream for the stream to reattach to the wall, the system becomes stable with a high gain. The further the wall are extended downstream of the reattachment region, the greater the bubble volume that is formed. Thus a greater control flow is required to expand the separation bubble to move the reattachment region beyond the end of the vent. If the setback of the boundary wall or the angle of the walls are increased the effect is similar to that for increasing the attachment wall length. As the wall is moved away from the stream, the size of separation bubble increases

a. Terminated-wall or bleed switching
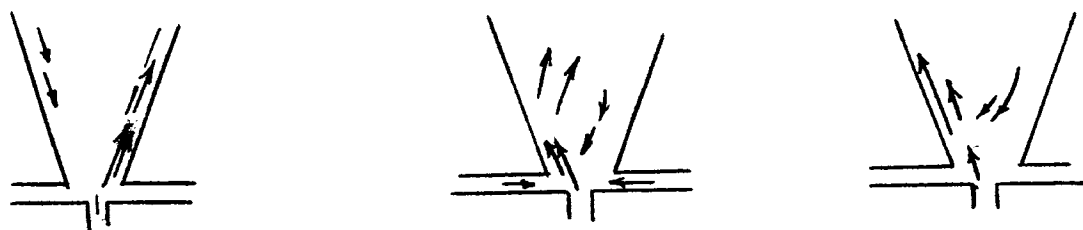
b. Contacting-both walls switching
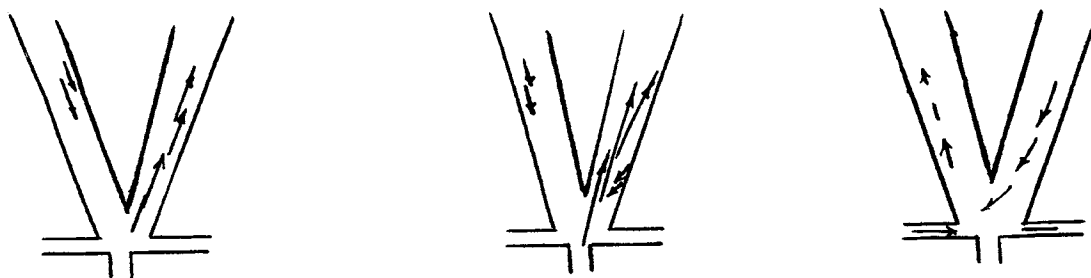
c. Splitter switching

Figure 3-2. Type of switching process(1)

and the reattachment region moves downstream closer to
the bleed of the wall. If the separation between the
walls and stream is increased still farther a condition is
reached where the stream will not attach to the side wall
of its own volition but instead a control flow is required
to obtain reattachment. Similarly increasing the angle of
the side wall to the stream leads to an increase in the
flow angle of attachment, and if the angle gets large
enough the stream will separate without a control flow.
Then an opposite control flow would also be needed to hold
the stream to the wall.

Contacting-both walls switching

This type of switching is the power jets contacting
the opposite wall while still in contact with the original
wall thus forming two separation bubbles prior to contac-
ting the splitter. Since the pressure in the separation
bubble is lower than on the unattached side of the stream,
a control flow is needed to raise the separation bubble
pressure and expand the bubble. This, in combination with
the momentum of the control stream causes the stream to
contact the opposite wall before it loses contact with
initial wall. Hence for a time there is a separation
bubble on both sides of the stream. However, control flow
into the initial separation bubble continues to expand it,
while entrainment contacts the opposite separation bubble.
The stream them progressively moves from one wall to the

other. Removing fluid through the control port (a suction)
on the opposite to which the stream is attached is a very
effective and efficient method of switching the stream in
this type of unit.

Splitter switching

This type of switching is characterized by the power
jet's contacting the splitter before contacting the opposite
wall and while still in contact with the initial wall.
When the splitter is positioned at the exit of the nozzle,
pipe flow prevails and the stream is split equally between
the outlets. This is a very stable situation. As the
splitter is moved downstream, the flow becomes more and
more bistable. For increased loading resistance (increasing
the output port restriction) a fluid amplifier having
splitter-type switching the pressure gain will also increase
up to the condition that will cause onset of oscillations
in the unit. The reason for this is that as the outputs
are constricted, the static pressure in the boundary layer
increases and assists in switching the stream.

Oscillator Circuit

An oscillating element can be designed from the basic
digital device in a number of ways. All of these variations
utilize some form of feedback to cause switching. There are
four different oscillator types as shown in Fig. 3-3.

1. feedback oscillator

2. coupled control oscillator

3. load sensitive oscillator

4. turbulence oscillator

Feedback oscillator

The feedback oscillator is shown in Fig. 3-3a. The output signal is fed back and applied as a negative signal at the amplifier control port. The oscillation frequency is determined by the transport time of the stream between the nozzle and receiver and by the passive component in the feedback paths.

A bistable amplifier exhibits a sawtooth characteristic in its feedback path as the pressure builds up to the switch level and then decays after the device changes state. Generally the transport time of the power jet from the nozzle to the output receiver is very small and the feedback impedance of this oscillator must include resistance and capacitance component to obtain sufficient phase shift for the oscillation to occur. The variable frequency characteristic then can be obtained by varying the feedback resistance or capacitance of the bistable device.

Coupled control oscillator

This device,which shown in Fig. 3-3b, is similar to the feedback type except it uses only one feedback loop, interconnecting the control ports. When the power jet

switches to one wall, a rarefaction wave is propaged in the control port at this side and a pressure wave develops in the control port on the opposite side. These waves traverse the connecting tube and when they arrive at the opposite control ports the power jet is switched. This device increases its frequency somewhat as the supply pressure is increased. Since the frequency of operation depends on the resistance and capacitance effects of the interconnected control ports, the frequency is very sensitive to changes in temperature. When the pressure is applied the resulting jet attaches itself to one of the sidewall, this introduces, by aspiration, a negative pressure in the control port on the attached sidewall, and this pressure forces fluid to move toward the low pressure control part. The time required to establish flow to the level that will release the power jet from the sidewall is then determined by the same transport time as indicated in feedback oscillator and response time of the passive network which couples the control port. By raising the supply pressure Ps a decrease in the pressure in the attachment bubble occurs and as result it increases the driving force in the interconnection line. This increased driving force is dominant and the time required to obtain the necessary flow to switch the element is decreased for high pressure signals.
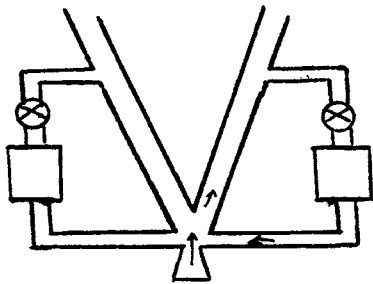
Load sensitive oscillator:

The load sensitive oscillator shown in Fig. 3-3c is
the same type of oscillator as provided in the feedback
device of Fig. 3-3a, except that the feedback path is
along the sidewall of the output passageway. Again, the
power stream signal flow establishes itself on one side-
wall and a negative pressure in the attachment bubble holds
the jet to the sidewall. However, in this element as the
pressure rises in the load output passage the attachment
bubble is separated and the power jet is released from the
wall. The jet then attaches itself to the opposite side-
wall and the sequence of events is repeated. In this type
of element the time required for the pressure to break the
attachment bubble is determined by the output leg volume
and the flow rates into the volume.

Turbulence oscillator:

The turbulence or Bell amplifier is also used as a
bistable element and changes state by a transition from a
laminar to a turbulence flow regime. This amplifier can be
made to oscillate by a simple feedback connection. The
output pressure is fed back as a control signal to cause
the laminar jet to become turbulent. When the jet is tur-
bulent, the output pressure is decreased. As the output
pressure falls the control signal is reduced below a certain
level and the jet returns to its laminar flow condition.

In evaluating all the possible variable frequency oscillators in the control circuit the classical feedback oscillator has demonstrated that it is sufficiently stable to perform the desired function. The coupled control port oscillator is relatively insensitive to signal pressure variation. This is because the increased driving force obtained by the decrease in the bubble pressure with increasing supply pressure is for the most part compensated by a requirement for a high switching flow level. The result is that no significant change in frequency occurs with increasing supply. The load sensitive oscillator by its very nature is insufficiently stable when coupled to another element which varies its load. In the turbulence amplifier the switching cycle is primarily governed by the recovery time of jet stream from the turbulent conditions. This is the predominent effect. The frequency of oscillations are far below any transport time that can be computed by the time constant of the feedback path, this element is rather insensitive to supply pressure changes. From the above evaluation the feedback oscillator appeared to offer easier operation and control of the frequency range. Therefore it was used for the bistable feedback oscillator in the later control circuit described in this paper.
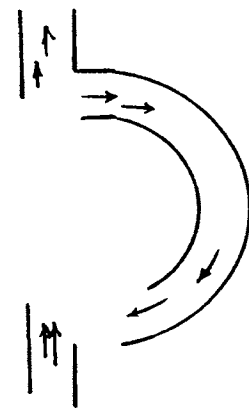
(a)   feedback oscillator
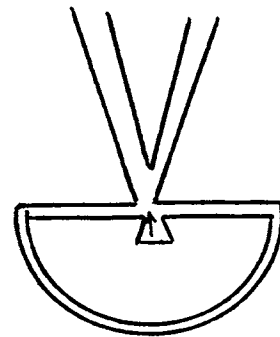
(b) coupled control
     oscillator
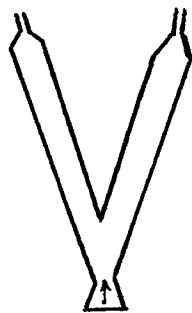
(c)   load sensitive oscillator

(d) turbulence
      oscillator

Figure 3-3. Fluid oscillator

Development of the Equation for Switching of the Amplifier

To investigate the switching time the following assumptions were made: (1) at the reattachment point the jet divides and (2) the shear forces are negligible compared with the jet momentum forces. The equations for estimating the switching level pressure are based on geometrical relations. (4), (20)

From Fig. 3-4b

$$\overline{X}_1 - \overline{X}_o = R(\alpha + \theta)$$

where $\overline{X}$ is the distance along the streamline and the reattachment angle θ is given by

$$R^1 = R \; Cos \; \theta.$$

Where
$$\frac{R^1}{R - L} = Cos \; \alpha$$

$$R \; Cos \; \theta = (R-L) \; Cos \; \alpha$$

$$Cos \; \theta = Cos \; \alpha \; (1 - \frac{L}{R})$$

$$\theta = Cos^{-1}(Cos \; \alpha(1 - \frac{L}{R})) \tag{1}$$

Here $R = \dfrac{L^2 + X^2 + 2LX \; Sin \; \alpha}{(L + X \; Sin \; \alpha)}$ \hfill (2)

The solution of radius R is presented in Appendix I.
From geometry the reattachment position is

$$X = \frac{R \, \text{Sin} \, (\alpha + \theta)}{\text{Cos} \, \alpha}$$

The volume, per unit depth, of the cavity between the jet centerline and the boundary walls is given by:

$$V = \frac{1}{2} \, (x+\theta) \cdot R^2 - \frac{1}{2}(R-L) \, R \, \text{Sin} \, (\alpha + \theta)$$

$$= \frac{1}{2}R^2 \, [(\alpha + \theta) - \frac{\text{Cos}\theta}{\text{Cos}\alpha} \, \text{Sin} \, (\alpha + \theta)]$$

The equation governing the behavior of the jet are assumed to be (1):

a) Velocity Profile

$$u = U \, \text{sech}^2 \eta$$

$$\text{Where } \eta = \frac{Y}{E_1 \overline{X}}$$

u = velocity of local point
U = velocity of jet at jet centerline
E_1 = entrainment rate for free jet

b) Momentum, J, per unit depth
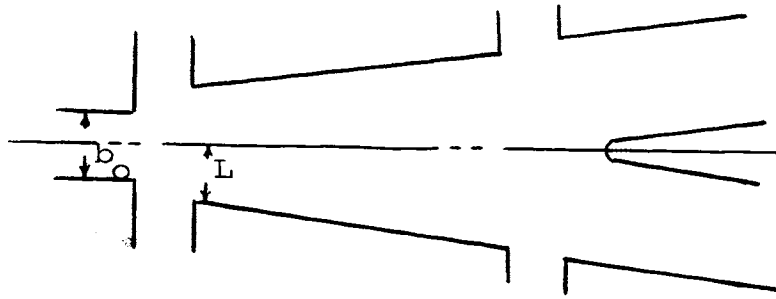
$$J = \frac{4}{3} \, \rho \, E \, \overline{X} \, u^2 = \text{Constant}$$

Here ρ is density of fluid, E is overall jet entrainment rate.
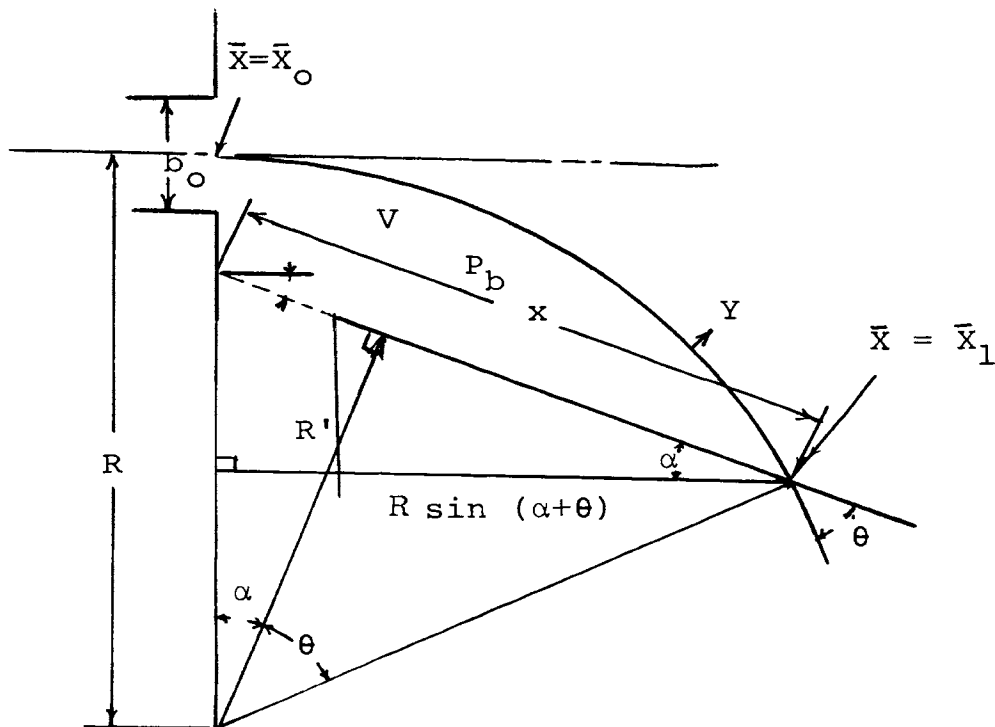
c) Volume, Q, per unit depth

$$Q = 2Eu\overline{X} = 2E\overline{X}U$$

$$Q_s = 2Eu_o\overline{X}_o = b_o u_o$$

a. Bleed type of switching bistable amplifier

b. Geometry of wall attachment jet

Figure 3-4. Geometry of wall attachment amplifier

Here Q_s is main flow in main jet exit.

$$J = \frac{4}{3} \rho E \overline{X}_o U_o^2$$

$$\overline{X}_o = \frac{b_o}{3E} \tag{5}$$

For the curved jet centerline jet path the radius of curvature of the path is defined as R, and the tangential velocity along the curved path is u. The infinitesimal element has a width dy(dR) and the mass of this element is

$$\rho \, dydA$$

Thus, the normal or radial acceleration is $\frac{u^2}{R}$ and the centrifugal force acting on the element has the magnitude $\rho \, dA \, dY \, (\frac{u^2}{R})$ across jet the pressure varies from P_b to $P_b + dP$ as the radius varies from R to R + dY. Since the shear force was assumed negligible, then the force balance in the radius direction is:

$$dAdP = \rho \, dA \, dY \, \frac{u^2}{R} \, .$$

Where $dA = R \, dY \, d\theta$ is differential cross section area.

$$\int_{P_b}^{P_\infty} dp = \frac{1}{R} \int \rho u^2 \, dy$$

$$P_\infty - P_b = \frac{J}{R} = \frac{\rho b_o u_o^2}{R} = \rho u_o^2 \, \frac{b_o}{R} = \frac{2bo}{R} \, (P_j - P_\infty)$$

$$-(\frac{P_b - P_\infty}{P_j - P_\infty}) = \frac{2bo}{R} = C_\Delta p \tag{6}$$

As $P_{bg} = P_b - P_\infty$, $P_{jg} = P_j - P_\infty$

$$-\frac{P_{bg}}{P_{jg}} = \frac{2bo}{R} = C_\Delta P$$

where P_j = absolute pressure of the power jet

P_∞ = atmosphere pressure

P_b = absolute pressure of bubble volume

P_{bg} = guage pressure of bubble volume

P_{jg} = guage pressure of power jet

Combining Eqs. 5 and 6 and Eq. for jet length, reattachment position

$$\frac{\overline{X}_l}{\overline{X}} = 1 + \frac{6E(\alpha+\theta)}{C_{\Delta p}} \qquad (7)$$

From Eq. 3 and Eq. 6

$$\frac{X}{b_o} = \frac{2}{C_{\Delta p}} \frac{\sin(\alpha + \theta)}{\cos \alpha} \qquad (8)$$

and from Eq. 4 the nondimension volume is

$$V^* = \frac{V}{b_o^2} = \frac{1}{2} \frac{R^2}{b_o^2} [(\alpha+\theta) - \frac{\cos\theta}{\cos\alpha} \sin(\alpha+\theta)]$$

$$V^* = \frac{2}{C_{\Delta P}^2} [(\alpha+\theta) - \frac{\cos\theta}{\cos\alpha} \sin(\alpha+\theta)] \qquad (9)$$

Eqs. 8 and 9 are important for investigating the switching characteristics. I can be seen by inspection of these equations that if a particular variable is specified, such as X/b_o then using Eq. 8 $C_{\Delta P} = f(X/b_o)$ and Eq. 9 $V* = f_1(C_{\Delta P}) = f_2(X/b_o)$. The relation of non-dimension volume and switching level, by using X/b_o as the independent parameter, is shown in Fig. 3-5. From the figure, it is found that increasing the length of the terminated wall causes an increase in the bubble volume, but decreases the required pressure switching level.

Development of the Equation for the Oscillator Circuit

The oscillator circuit has been schematically shown in Fig. 3-3a. Where the electric symbols represent a resistance and capacitance in the feedback path. In order to simplify the mathematics of the analysis of the system of the feedback oscillator circuit the following assumptions are made:

a) the feedback resistance R_f and the control port resistance Rc are considered to be constants, and let Rc = nRf

b) the output pressure Po of the bistable amplifier and the bubble pressure Pc are considered uniform.

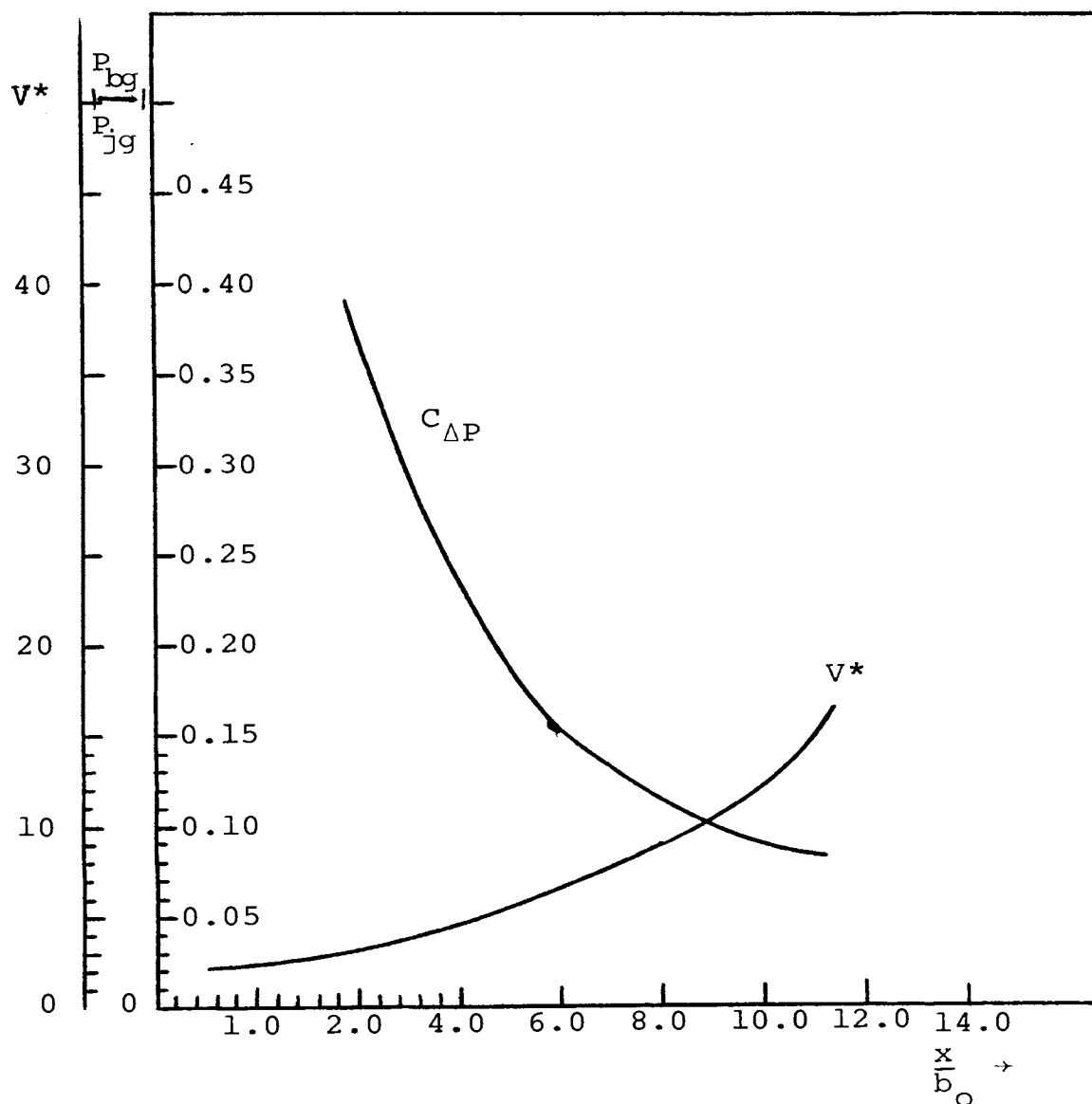c) the inductance in the transmission line is assumed negligibly small.

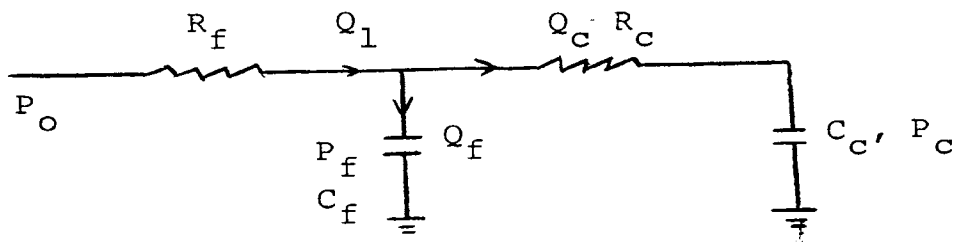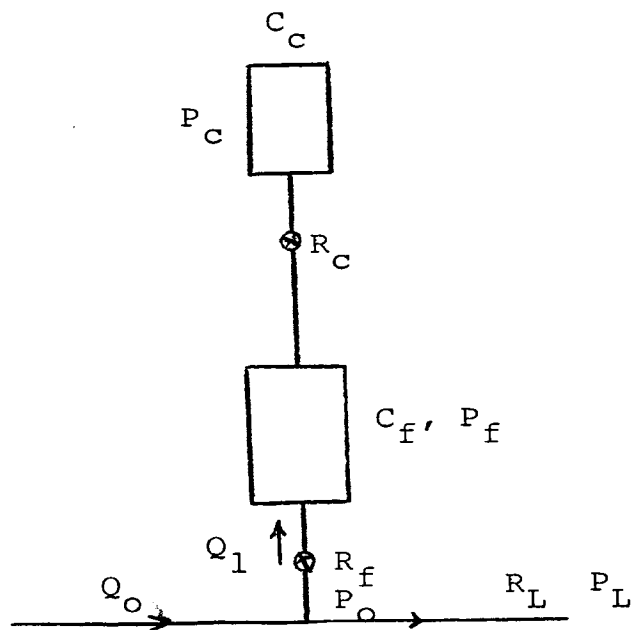Figure 3-5.   Relation of $C_{\Delta P} = f(\frac{x}{b_o})$ and $V^* = f(\frac{x}{b_o})$

Figure 3-6. Equivalent electric circuit of feedback path

The equivalent electric circuit is shown in Fig. 3-6. From the diagram,

$$Q_1 = Q_c + Q_f \qquad (10)$$

$$Q_c = Q_1 - Q_f$$

$$Q_1 = \frac{P_o - P_f}{R_f} \quad \text{and} \quad Q_f = C_f \frac{dP_f}{dt} \qquad (11)$$

Where $C_f = \dfrac{V_f}{kP_{fa}}$ for isothermal condition $k = 1$ and P_{fa} is the mean absolute pressure in the feedback capacitance

$$Q_c = \frac{P_f - P_c}{R_c} = C_c \frac{dP_c}{dt} \qquad (12)$$

Where $C_c = \dfrac{V}{P_{ba}}$ for isothermal condition

Here V is the bubble volume, and P_{ba} is the absolute mean bubble pressure.

Initially it will be assumed that C_c and C_f can be represented by constants evaluated at a mean value. This solution will then be compared with the case wherein the variations in C_f and C_c with pressure and bubble volume are considered.

Combining Eqs. 10, 11, 12,

$$C_f \frac{dP_f}{dt} + (\frac{1}{Rf} + \frac{1}{Rc}) P_f = \frac{Po}{Rf} + \frac{Pc}{Rc} \qquad (13)$$

and

$$R_c C_c \frac{dP_c}{dt} + P_c = P_f \qquad (14)$$

Eliminating P_f between Eqs. 13 and 14 gives

$$R_f C_f R_c C_c \frac{d^2 P_c}{dt^2} + (R_c C_c + R_f C_c + R_f C_f) \frac{dP_c}{dt} + P_c = P_o$$

Let $R_f C_f = \tau_f$ and $R_c C_c = \tau_c$ for convenience, so

$$\tau_f \tau_c \frac{d^2 P_c}{dt^2} + (\tau_f + \tau_c + R_f C_c) \frac{dP_c}{dt} + P_c = P_o \qquad (15)$$

$R_f C_c$ has the dimension of time but has no physical significance in Eq. 15 in terms of a volume time constant. The 2nd order equation can be factored to give two effective time constants, since as shown below, the damping coefficient is always greater than 1.

$$(\frac{1}{\omega_n})^2 = \tau_f \tau_c \qquad\qquad \omega_n = \frac{1}{\sqrt{\tau_f \tau_c}}$$

$$\frac{2\xi}{\omega_n} = \tau_f + \tau_c + R_f C_c$$

$$\xi = \frac{\tau_f + \tau_c}{2\sqrt{\tau_f \tau_c}} + \frac{R_f C_c}{2\sqrt{\tau_f \tau_c}}$$

τ_f, τ_c, R_f and C_c is real value and $(\tau_f + \tau_c + R_f C_c)^2 - \tau_f \tau_c > 0$, so $\xi > 1$. So the equation can be written as

$$(\tau_{fe} D + 1)(\tau_{ce} D + 1) P_c = P_o \qquad (16)$$

Where τ_{fe} and τ_{ce} in Eq. 16 are effective time constants. If $R_f << R_c$ and $C_c << C_f$, the product $R_f C_c$ then is much smaller than $\tau_f + \tau_c$; thus, if $R_f C_c$ can be neglected,

$$\tau_{fe} = \tau_f \quad \text{and} \quad \tau_{ce} = \tau_c$$

In this case, the transient response of P_c to constant working output pressure P_o is

$$P_c = P_o [1-(1-\frac{\tau_c}{\tau_f})e^{-t/\tau_f} + (\frac{\tau_f}{\tau_c} - 1)e^{-t/\tau_c}] \qquad (17)$$

$$= P_o \{1 - [(1-\frac{\tau_c}{\tau_f})e^{-t/\tau_f} - (\frac{\tau_f}{\tau_c} -1)e^{-t/\tau_c}]\} \qquad (18)$$

$$= P_o \{1-(e^{-t/\tau_f} + e^{-t/\tau_c})+(\frac{\tau_c}{\tau_f}e^{-t/\tau_f} + \frac{\tau_f}{\tau_c}e^{-t/\tau_c})\}$$

Since $C_c = f_1 (V, P_c) = f_2(\frac{x}{bo}) = f_2(P_c)$ the variation between C_c and P_c is shown in Figs. 3-7, 3-8. The approximated equation of $C_c = f(P_c)$ gotten from Fig. 3-8 for the range $P_c/P_s = 0.1$ to $P_c/P_s = 0.30$ is

$$C_c P_c = 0.280 \times 10^{-4} \times P_s$$

the average value of C_c is $C_c = 1.72 \times 10^{-4} \frac{in^5}{lb\ sec}$, this is very small compared with realistic values of C_f, hence the ratio of time constants,

$$\frac{\tau_f}{\tau_c} = \frac{R_f C_f}{R_c C_c} = \frac{C_f}{n\, C_c} > 10^3$$

This makes the transient response more like that of a single first order element.

With $\frac{\tau_f}{\tau_c} > 10^3$ the terms e^{-t/τ_c}, $\frac{\tau_c}{\tau_f} e^{-t/\tau_f}$, and $\frac{\tau_f}{\tau_c} e^{-t/\tau_c}$ are much smaller than e^{-t/τ_f}, so the transient response can be approximately reduced to

$$P_c = P_o [1 - e^{-t/\tau_f}] \tag{19}$$

The solution of Eq. 18 same as Eq. 19 comparing with the completed solution which includes the variation of C_c, and C_f is shown in Fig. 3-9. From this shows that approximated solution is satisfied with the assumption.

After the first cycle of operation, there is an initial pressure in the capacitance C_f, so Eqs. 10, 11, 13 and 14 can be rearranged as:

$$Q_1 = \frac{P_o - (P_f + P_{fo})}{R_f} \tag{20}$$

$$Q_c = \frac{(P_f + P_{fo}) - P_c}{R_c} = C_c \frac{dP_c}{dt} \tag{21}$$

$$Q_f = C_f \frac{dP_f}{dt}$$

$$Q_f = Q_1 - Q_c$$

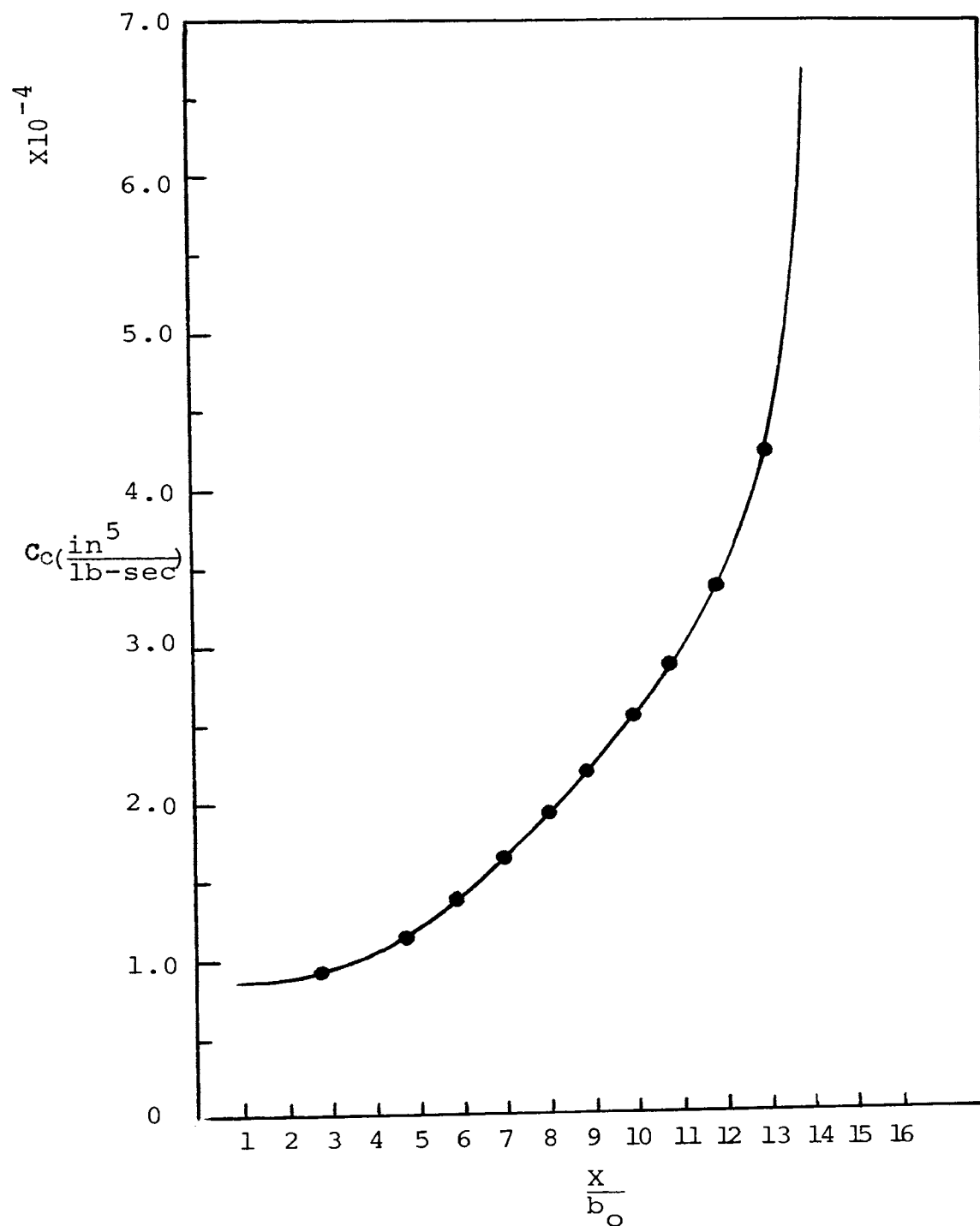$$C_f \frac{dP_f}{dt} = \frac{P_o - (P_f + P_{fo})}{R_f} - \frac{(P_f + P_{fo}) - P_c}{R_c}$$
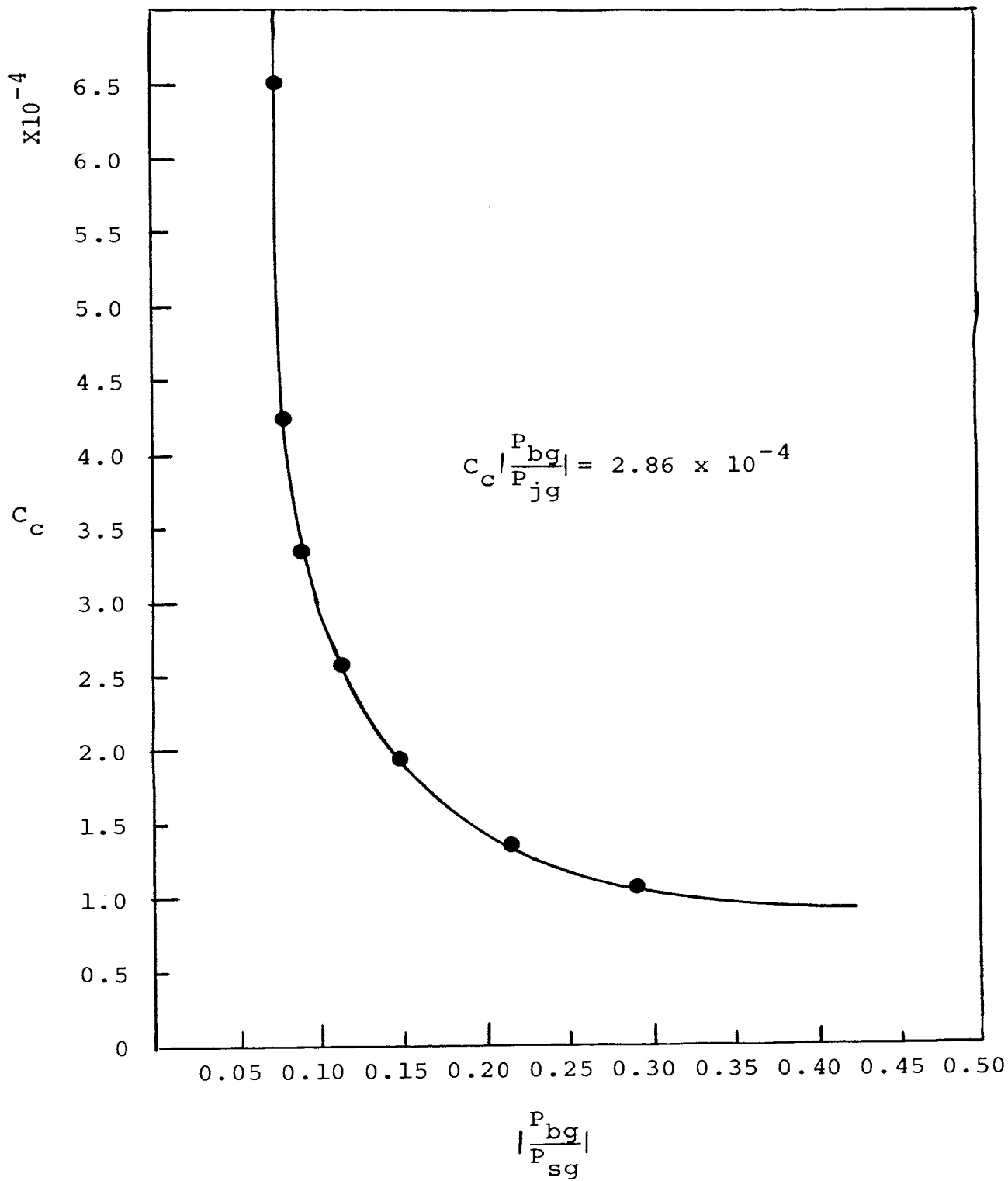
Figure 3-7. Relation between C_c and $\frac{X}{b_o}$

Figure 3-8. Variation between C_c and P_c

$$C_f \frac{dP_f}{dt} + (\frac{1}{R_f} + \frac{1}{R_c}) \, P_f = \frac{P_o}{R_f} + \frac{P_c}{R_c} - (\frac{1}{R_f} + \frac{1}{R_c}) P_{fo} \qquad (22)$$

$$C_f \frac{dP_f}{dt} + (\frac{1}{R_f} + \frac{1}{R_c}) (P_f + P_{fo}) = \frac{P_o}{R_f} + \frac{P_c}{R_c} \qquad (23)$$

and

$$R_c C_c \frac{dP_c}{dt} + P_c = P_f + P_{fo}$$

$$P_f = R_c C_c \frac{dP_c}{dt} + P_c - P_{fo}$$

$$\frac{dP_f}{dt} = R_c C_c \frac{d^2 P_c}{dt^2} + \frac{dP_c}{dt} - \frac{dP_{fo}}{dt}$$

From which

$$\tau_f \tau_c \frac{d^2 P_c}{dt^2} + (\tau_f + \tau_c + R_f C_c) \frac{dP_c}{dt} + P_c = P_o + \tau_f \frac{dP_{fo}}{dt}$$

is reduced to

$$\tau_f \tau_c \frac{d^2 P_c}{dt^2} + (\tau_f + \tau_c) \frac{dP_c}{dt} + P_c = P_o + \tau_f \frac{dP_{fo}}{dt} \qquad (24)$$

where the term $\frac{dP_{fo}}{dt}$ is the slope at the initial starting point of the second cycle.

The slope of P_f response curve at the end of first empting cycle and at the start of second filling cycle can be determined from equation 22 by setting Pc = 0. Therefore,
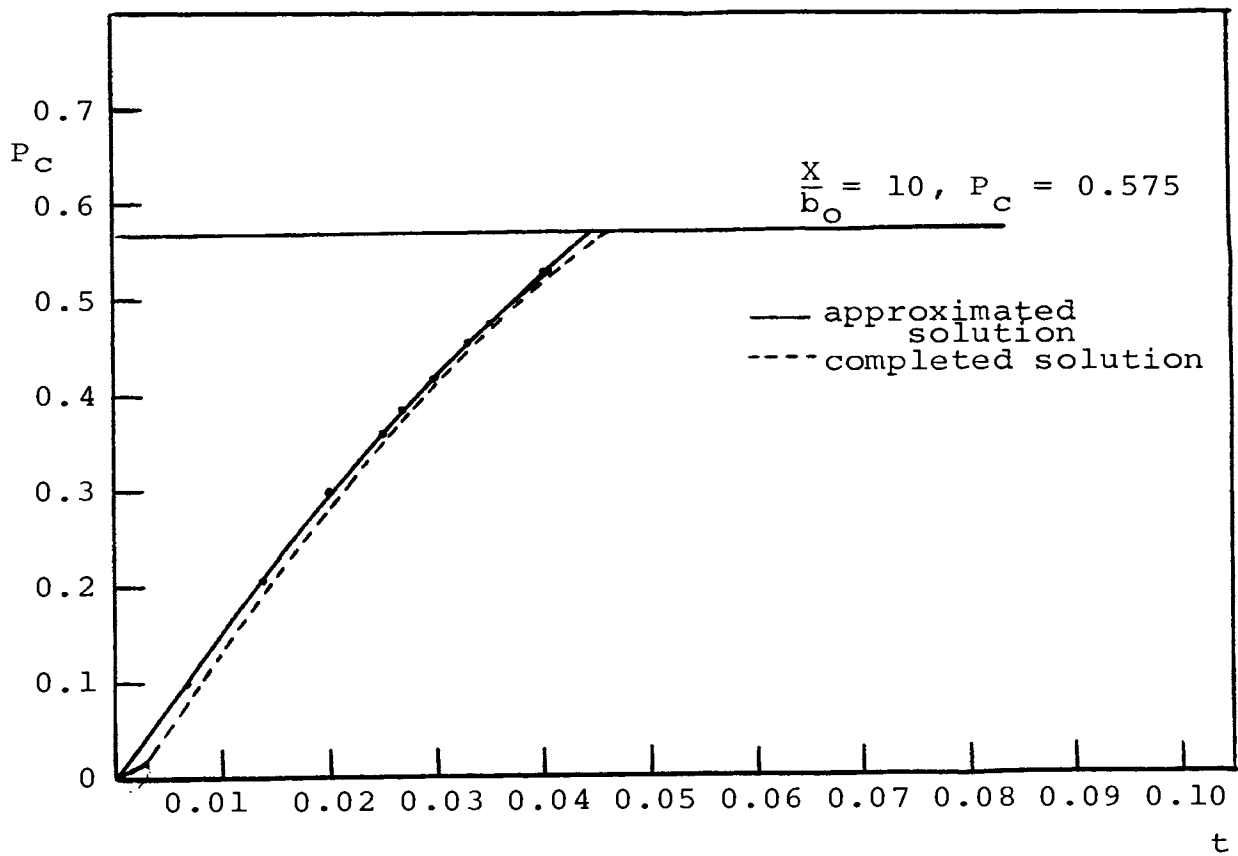
Figure 3-9a.   Comparison between completed and
               approximated solution of P_C response
               in first cycle
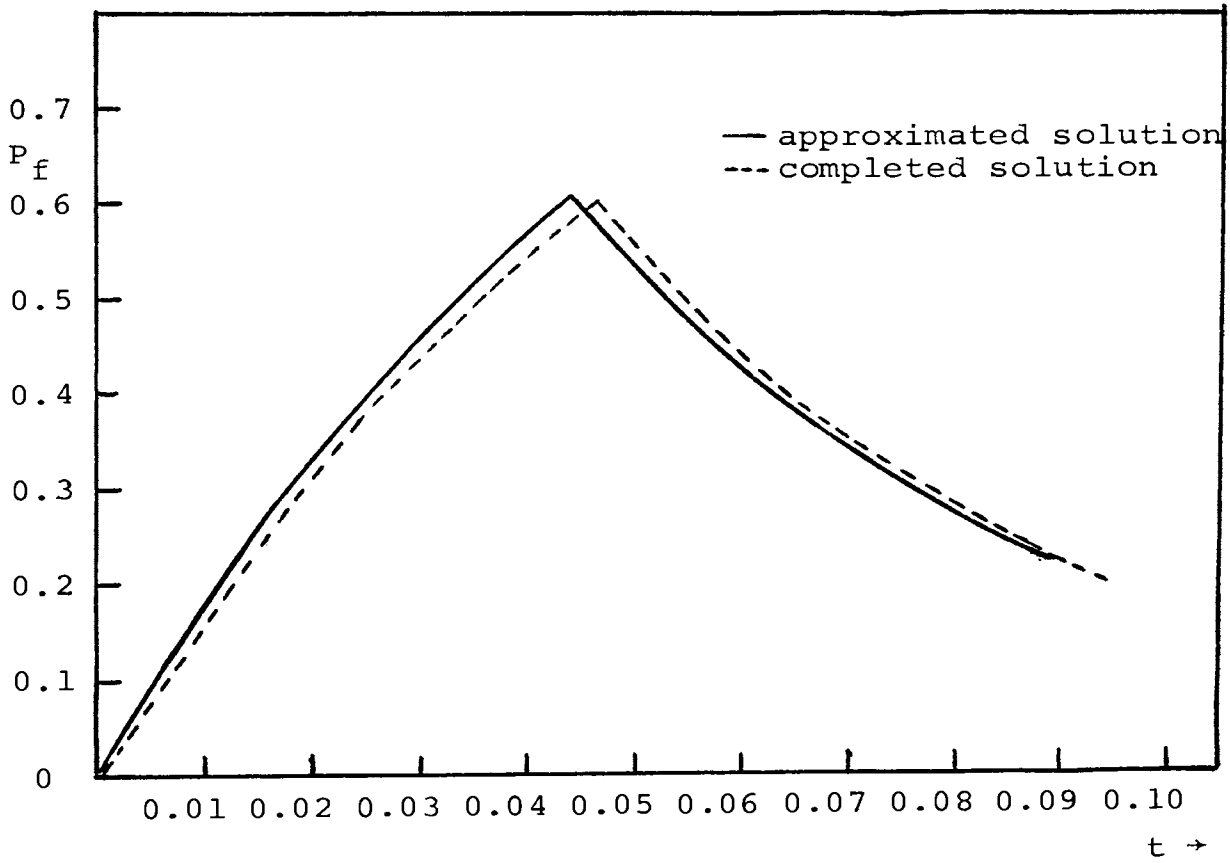
Figure 3-9b.   Comparison between completed and
approximated solution of P_f response
in first cycle

the Eq. 22 becomes

$$Cf \frac{dP_f}{dt} + (\frac{1}{R_f} + \frac{1}{Rc}) P_f = \frac{P_o}{R_f} - (\frac{1}{R_f} + \frac{1}{R_c}) P_{fol}$$

$$\tau_f \frac{dPf}{dt} + \frac{n+1}{n} P_f = P_0 - \frac{n+1}{n} P_{fol}$$

Solving the equation

$$P_f = \frac{n}{n+1} P_o [1 - e^{-\frac{(n+1)}{n} \frac{t}{\tau_f}}] - P_{fol}$$

$$\frac{dP_f}{dt} = \frac{P_o}{\tau_f} e^{-\frac{(n+1)}{n} \frac{t}{\tau_f}} - \frac{dP_{fol}}{dt}$$

$$[\tau_f \frac{dP_f}{dt}]_{t=0} = [P_o]_{t=0} - [\tau_f \frac{dP_{fol}}{dt}]_{t=-0}$$

Where $\frac{dPf}{dt}$ is the slope at the starting point of second cycle, when $t \to +0$ and $\frac{dPfol}{dt}$ is the slope of the ending point of the first empting cycle.

After switching, the capacitance C_f is discharged through the resistance R_f and Rc, and the response of Pf in discharging process is:

$$Cf \frac{dPf}{dt} + (\frac{1}{Rf} + \frac{1}{Rc}) Pf = 0$$

$$P_f = P_{fp} \, e^{-\left(\frac{1}{R_f} + \frac{1}{R_c}\right)\frac{t}{C_f}} = P_{fp} \, e^{-\frac{n+1}{n}\frac{t}{\tau_f}} \qquad (25)$$

Where P_{fp} is the peak pressure in capacitance when switching starts. From Eqs. 23, 24 and 25 the non-dimensional response of Pc and Pf of each cycle is shown in Fig. 3-10, 3-11, and the oscillating period thus can be found when the response of Pf reaches the steady range.

The plot of approximated solution and completed solution of first cycle by selecting the value, $R_f = 0.2$, $R_c = 0.4$, $P_s = 5$ psig, and $\frac{P_o}{P_s} = 0.23$ is shown in Fig. 3-9, it shows that the approximated solution is sufficient in determining the oscillation period. Then from Figs. 3-5, 3-10 and 3-11 a non-dimensional relationship between the time and pressure can be derived for convenience in determining the oscillation period. In order to determine the particular oscillation frequency, the characteristics of Cf must be known, as capacitance volume Vf is constant, and so Cf varies only with Pf, by using the average pressure Pfa, from Fig. 3-11,

$$\frac{Pfa}{Ps} = 0.092 \quad \text{for} \quad \frac{P_o}{P_s} = 0.23 \quad \text{and} \quad P_s = 5 \text{ psig}$$

The resulting between Pf and Cf is shown in Fig. 3-13, from this figure the Cf is almost constant although the Pf varies. Using the above results, if the supply pressure Ps, resistance Rf, capacitance volume Vf and the design data of the
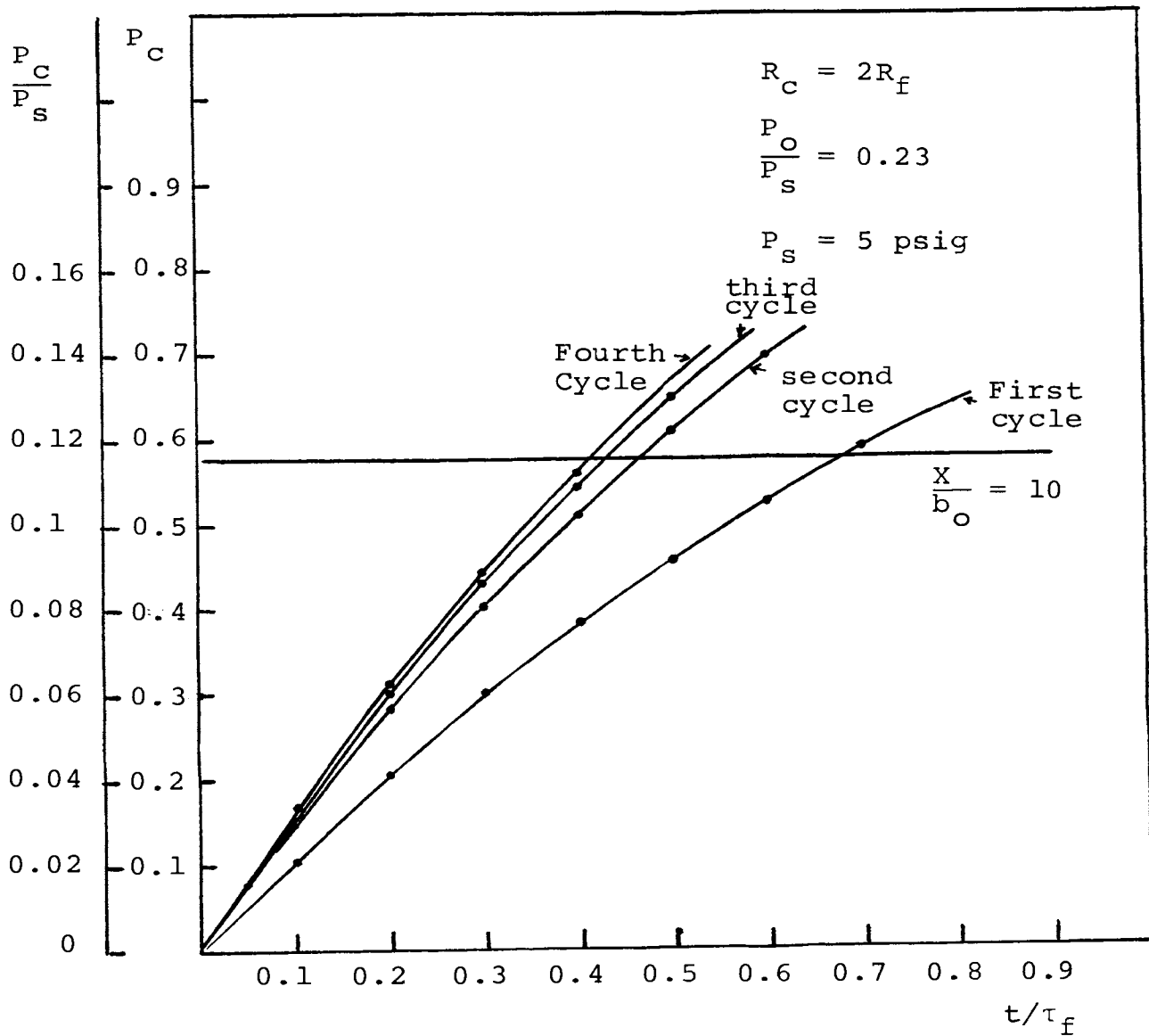
Figure 3-10. Response of non-dimension time and pressure of first four cycles operation
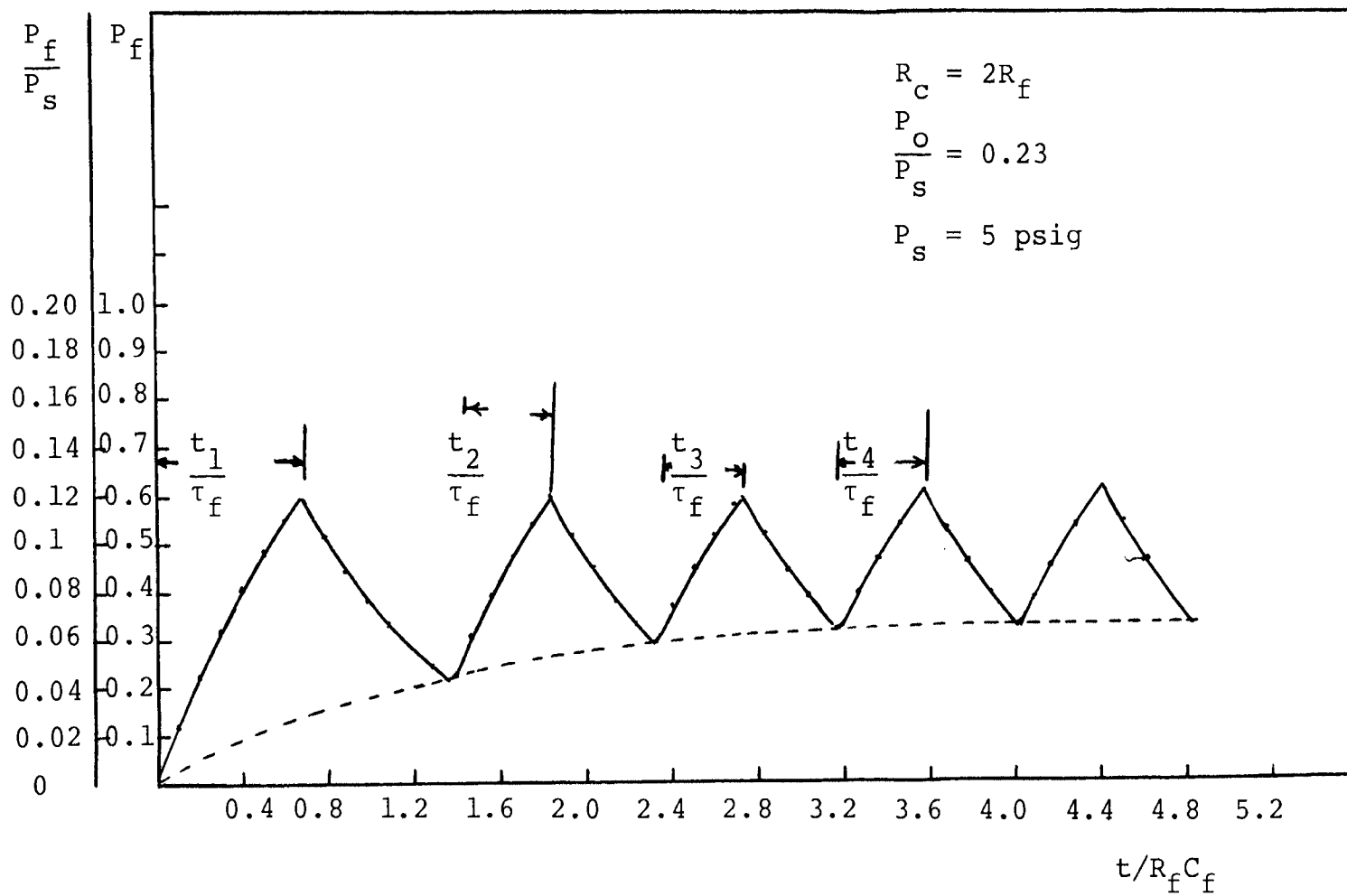
Figure 3-11. Response of capacitance pressure in feedback path
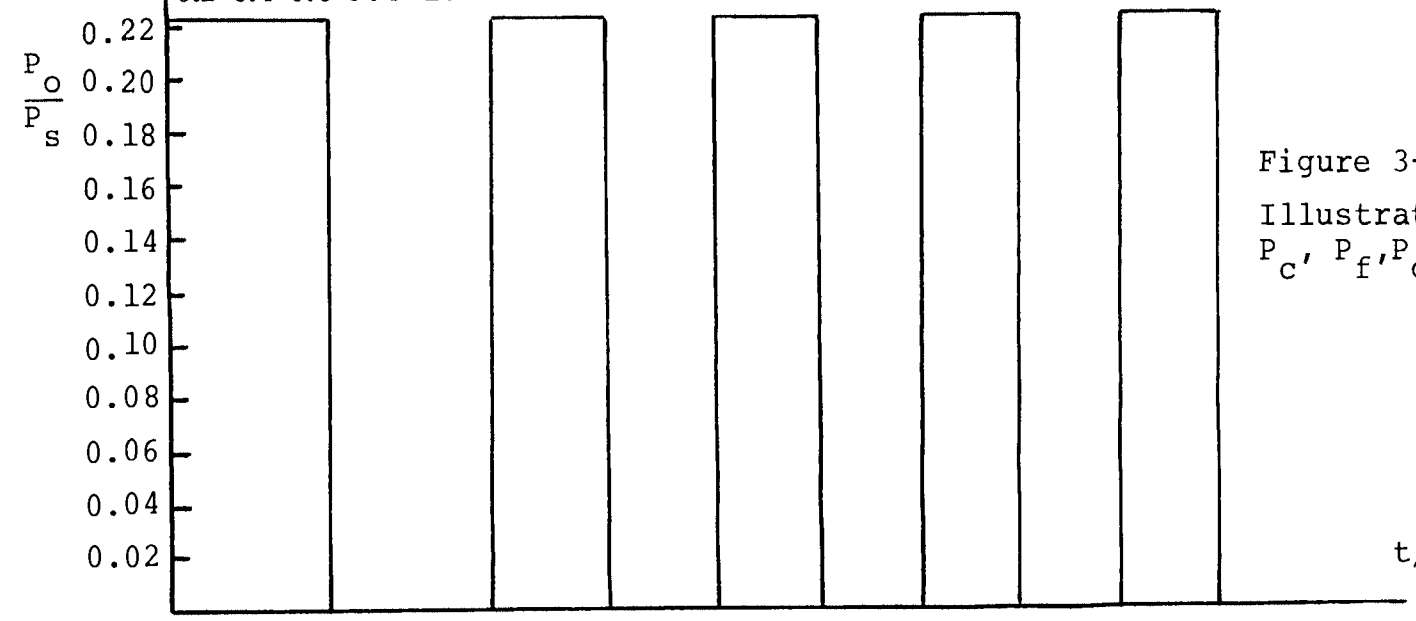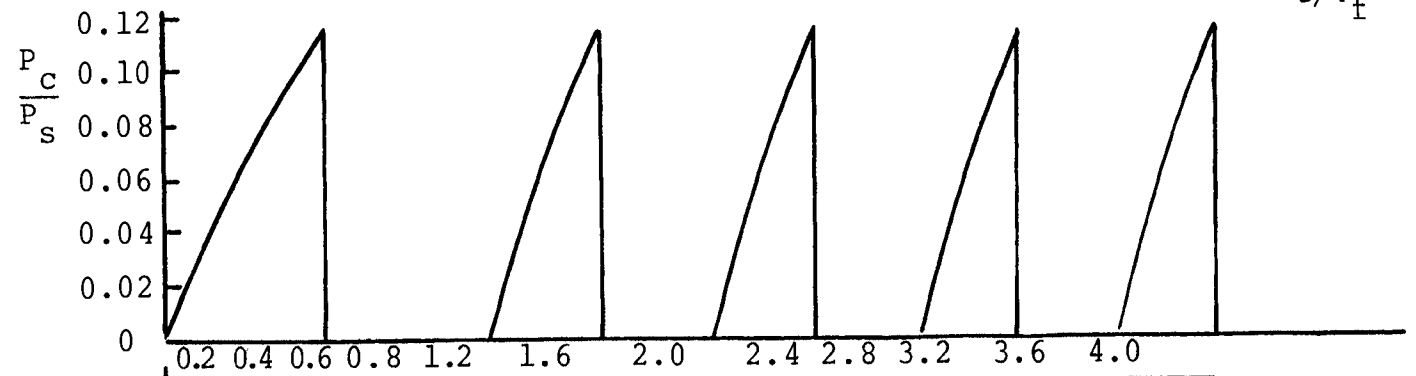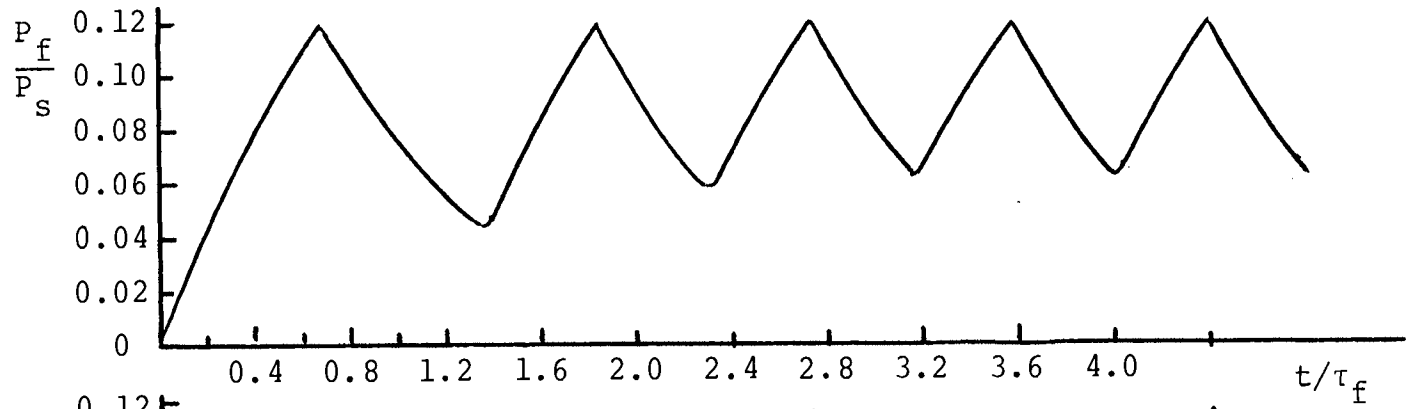
Figure 3-12:

Illustration of P_c, P_f, P_o Response
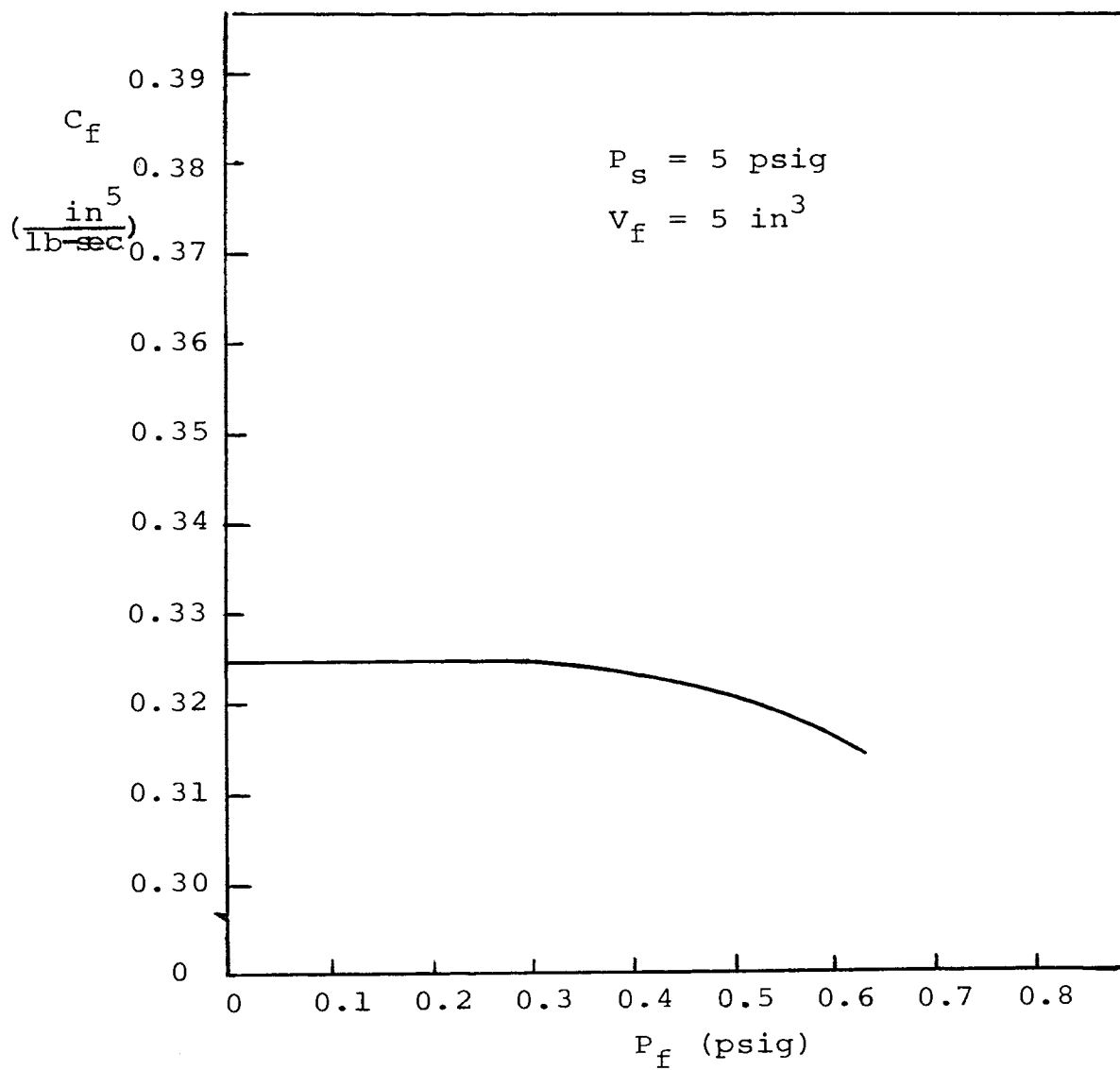
Figure 3-13. Variation between C_f and P_f

amplifier is known, then the oscillation period can be determined from Figs. 3-5, 3-9, and 3-10. Let Ps = 5 psig $\frac{P_o}{P_s}$ = 0.23, Rf = 0.2 $\frac{lb\text{-}sec}{in^5}$, Vf = 5 in^3, b_o = 0.02 in and distance of bleed X = 0.2 in.

Then with $\frac{X}{b_o}$ = 10 from Fig. 3-5. $\frac{Pbg}{Ps}$ = 0.115

thus, $\frac{t}{R_f C_f}$ = 0.415

$$C_f = \frac{5}{0.092 \times 5 + 14.67} = 0.33 \frac{in^5}{lb\ sec}$$

$$t = 0.415 \times 0.2 \times 0.33 = 0.0275\ sec$$

So the oscillation period tos is

$$tos = 2t + 2tl$$

Where tl is the transport time of amplifier; $t_1 = \frac{x2}{uo}$ = 0.0002, where X2 is the distance between the nozzle and receiver, generally t_1 is much smaller compared to t, so roughly calculated oscillation period:

$$tos = 2t = 2 \times 0.0275 = 0.055\ sec, \text{ and frequency}$$

f = 18 cps.

Up to this point the effect of variation of the amplifier output load has not been investigated. Suppose there is a load resistance R_L in the output line, and P_{01} is the out pressure of the bistable amplifier.

From Fig. 3-14

$$Q_o = Q_{co} + Q_1 + Q_2$$

where

$$Q_{co} = C_o \frac{dP_o}{dt}$$

$$Q_2 = \frac{P_o}{R_L}$$

$$Q_1 = \frac{P_o - P_f}{R_f} \qquad Q_o = \frac{P_{01} - P_o}{R_o}$$

$$\frac{P_{01}}{R_o} = C_o \frac{dP_o}{dt} + \left(\frac{1}{R_L} + \frac{1}{R_o} + \frac{1}{R_f}\right) P_o - \frac{P_f}{R_f} \qquad (26)$$

Substitute Eqs. 14 and 16 to Eq. 26.

$$\frac{P_{01}}{R_o} = \left(\frac{1}{R_L} + \frac{1}{R_o} + \frac{1}{R_f}\right) \left[\tau_f \tau_c \frac{d^2 P_c}{dt^2} + (\tau_f + \tau_c) \frac{dP_c}{dt} + P_c\right]$$

$$+ C_o \left[\tau_f \tau_c \frac{d^3 P_c}{dt^3} + (\tau_f + \tau_c) \frac{d^2 P_c}{dt^2} + \frac{dP_c}{dt}\right] - \frac{\tau_c \frac{dP_c}{dt} + P_c}{R_f}$$

From the previous analysis, $\frac{\tau_f}{\tau_c} > 10^3$, $\tau_c \ll \tau_f$. By using the order magnitude analysis the equation can be reduced to:

$$\frac{P_{01}}{R_o} = C_o \tau_f \frac{d^2 P_c}{dt^2} + \left[\left(\frac{1}{R_L} + \frac{1}{R_o} + \frac{1}{R_f}\right) \tau_f + C_o\right] \frac{dP_o}{dt}$$

$$+ \left(\frac{1}{R_L} + \frac{1}{R_o}\right) P_c$$
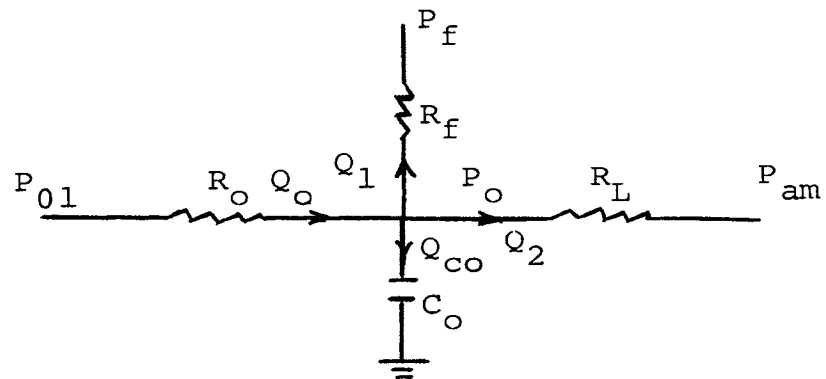
Figure 3-14. Equivalent electric circuit in output line

$$\tau_o \tau_f \frac{d^2 P_c}{dt^2} + [(\frac{R_o}{R_L} + 1)\tau_f + \tau_o + T_o C_f] \frac{dP_c}{dt} + (\frac{R_o}{R_L} + 1)$$

$$P_c = P_{01} \tag{27}$$

Where $\tau_o = R_o C_o$ and $R_o C_f$ has the dimension of time but no physical significance in equation 27, so Eq. 27 could be written as:

$$\tau_o \tau_f \frac{d^2 P_c}{dt^2} + [(\frac{R_o}{R_L} + 1)\tau_f + \tau_o] \frac{dP_c}{dt} + (\frac{R_o}{R_L} + 1)P_c = P_{01} \tag{28}$$

The general solution of Eq. 28 is

$$P_c = \frac{P_{01}}{\frac{R_o}{R_L} + 1} [1 - A e^{-\frac{t}{C_o R_L R_o}{R_L + R_o}} - B e^{-t/\tau_f} \tag{29}$$

Where

$$A = \frac{\tau_o R_L}{(R_o + R_L)\tau_f - \tau_o R_L}$$

$$B = \frac{\tau_f R_L}{\tau_o R_L - (R_o + R_L)\tau_f}$$

From Eq. 29, the response of control pressure P_c is a function of the load resistance R_L, feedback resistance R_f, feedback capacitance C_f and supply pressure P_s. The effect of an increment increase in load resistance is to increase the asymtotic value $\frac{P_{01}}{\frac{R_o}{R_L} + 1}$ and the intersection

with the switching pressure for a shorter time.

As for the bistable amplifier, and therefore its output characteristic $(P_{01} = P_{01}(Q_s))$, it is noticed than an increase of supply flow Q_s results in a faster response. Thus to vary Q_s for a given element, the supply pressure could be changed and therefore also the value of switching level.

The result of the variation of supply pressure will then depend on the mutual importance of all these factors. However, the increasing of the supply pressure and the resulting increment of switching level becomes the primary factor effecting the oscillating period.

IV. SUMMARY AND CONCLUSION

A primary component in the development of many control systems is the bistable oscillator which provides the oscillating frequency to control the position system or provide the time sequence. The theoretical equations and solutions were shown in this paper. The important parameters effecting the oscillation are feedback resistance, capacitance, bistable amplifier supply pressure, and the geometry and dimension of the bistable amplifier. The non-dimensional time and pressure response were based on approximated solution of Eqs. 18, 24 and 25 as shown in Fig. 3-10, and 3-11. The determination of oscillation period, being found after four cycles of operation, was based on the characteristics of the bistable amplifier and feedback path. The variations in frequency as a result of varying the feedback resistance R_f of capacitance C_f can also be calculated.

In order to reduce the inaccuracy of the position actuator system, the range of frequency should be considered. The oscillation frequency for particular values of the various system parameters was found from Fig. 3-10. However, the actual operating frequency is more dependent on the servo valve. This work remains to be done in the area of theoretical approach of the behavior of the diaphragm which connects the sampling device and servo valve.

The result of the analysis in this paper was based on the "lumped parameter" approach, the assumption of a constant pressure throughout the pneumatic transmission line was made. But for higher frequency operation, the long transmission lines may have a significant transport delay and/or a significant phase lag and amplitude attenuation in transmitting signals, thus the use of "distributed parameter" analysis should also be considered.

From the results of this lumped parameter analysis, the theoretical behavior of bistable oscillator was investigated and the non-dimensional results were set for convenience in determining the oscillation period.

V. APPENDIX I
Solution of radius of curvature R

Take the trigonometeric identify

$$\tan(\frac{\alpha+\theta}{2}) = \frac{1-\cos(\theta+\alpha)}{1+\cos(\theta+\alpha)}$$

Use the geometric relation

$$\tan(\frac{\alpha+\theta}{2}) = \frac{L+X\ \sin\alpha}{X} \qquad X_L = X\cos\alpha$$

$$(\frac{L+X\ \sin\alpha}{X_L})^2 = \frac{1-\cos(\theta+\alpha)}{1+\cos(\theta+\alpha)}$$

$$= \frac{1-\dfrac{R-(L+X\ \sin\alpha)}{R}}{\dfrac{R-(L+(L+X\ \sin\alpha))}{R}}$$

$$= \frac{L+X\ \sin\alpha}{2R-(L+X\ \sin\alpha)}$$

So,

$$\frac{L+X\ \sin\alpha}{X_L^2} = \frac{1}{2R-(L+X\ \sin\alpha)}$$

$$2R(L+X\ \sin\alpha) = X_L^2 + (L+X\ \sin\alpha)^2$$

$$= (X\cos\alpha)^2 + L^2 + 2LX\ \sin\alpha + (X\ \sin\alpha)^2$$

$$= X^2 + L^2 + 2LX\ \sin\alpha$$

$$R = \frac{X^2 + L^2 + 2LX\ \sin\alpha}{2(L+X\ \sin\alpha)}$$
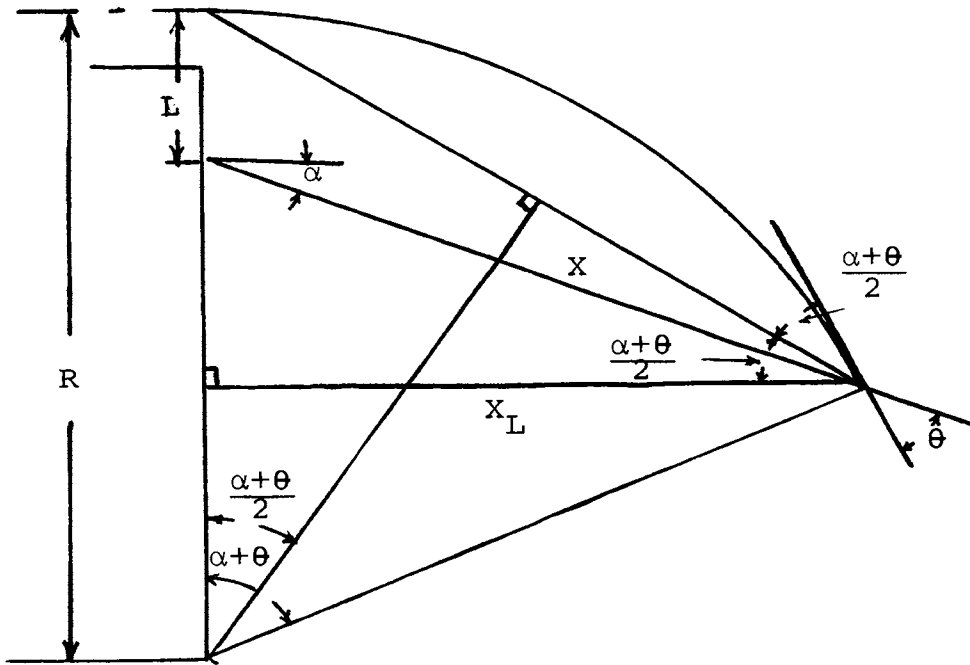
Figure A-1.   Geometrical configuration of
attaching jet

VI. APPENDIX II

Table 1. Calculation of bistable amplifier switching pressure level

$\dfrac{X}{b_o}$	R	$\cos\theta$	θ	$-C_{\Delta P}$	V*	C_c	$-P_c$
2	0.0428	0.59	53.9	0.935	2.06	0.824×10^{-4}	4.675
3	0.0668	0.731	47.0	0.596			2.98
4	0.108	0.825	34.26	0.370			1.850
5	0.137	0.856	31.0	0.292	3.53	1.07×10^{-4}	1.460
6	0.185	0.898	26.0	0.216	4.59	1.34×10^{-4}	1.080
7	0.215	0.900	25.6	0.186	5.63	1.64×10^{-4}	0.930
8	0.270	0.9163	23.58	0.149	6.75	1.94×10^{-4}	0.745
9	0.302	0.922	22.66	0.132	7.50	2.14×10^{-4}	0.660
10	0.360	0.931	21.33	0.115	8.92	2.53×10^{-4}	0.575
11	0.400	0.935	20.66	0.103	10.01	2.83×10^{-4}	0.515
12	0.446	0.941	19.66	0.090	11.9	3.34×10^{-4}	0.45
13	0.490	0.946	18.66	0.0816	15.00	4.20×10^{-4}	0.408
14	0.740	0.954	17.3	0.0540	23.188	6.49×10^{-4}	0.27

VII. APPENDIX III

Calculation of bubble pressure and feedback capacitance pressure response to constant working output pressure

<u>Table II</u>. Calculation of response pressure P_c, P_f and discharge pressure P_{fo} in first cycle

$\dfrac{t_1}{\tau_f}$	0	0.1	0.2	0.3	0.4	0.5	0.6	0.58	0.7
P_c	0	0.101	0.208	0.30	0.381	0.454	0.523	0.575	0.584
P_f	0	0.120	0.2274	0.323	0.4088	0.486	0.555	0.601	0.616
P_{fo} (discharge)		0.517	0.434	0.384	0.331	0.282	0.2445	0.221	0.210

<u>Table III</u>. Calculation of response pressure P_c, P_f and discharge P_{fo} in second cycle

$\dfrac{t_2}{\tau_f}$	0	0.1	0.2	0.3	0.4	0.47	0.5
P_c	0	0.148	0.2812	0.401	0.508	0.575	0.605
P_f	0.221	0.310	0.3925	0.4686	0.5397	0.60	0.603
P_{fo} (discharge)	0.514	0.443	0.381	0.328	0.291	0.279	

Table IV. Calculation of response pressure P_c, P_f and discharge pressure P_{fo} in third cycle

$\dfrac{t_3}{\tau_f}$	0	0.1	0.2	0.3	0.4	0.43	0.5
P_c	0	0.1586	0.3004	0.429	0.547	0.575	0.6488
P_f	0.291	0.370	0.444	0.5139	0.5791	0.60	0.6396
P_{fo} (discharge)	0.518	0.439	0.384	0.331	0.315	0.282	

Table V. Calculation of response pressure P_c, P_f and discharge pressure P_{fo} in fourth cycle

$\dfrac{t_4}{\tau_f}$	0	0.1	0.2	0.3	0.4	0.415	0.5
P_c	0	0.1623	0.308	0.439	0.557	0.575	0.663
P_f	0.315	0.3908	0.4626	0.530	0.593	0.60	0.652
P_{fo} (discharge)	0.52	0.449	0.386	0.33	0.317	0.282	

VIII. BIBLIOGRAPHY

1. Kirshner, Joseph M. "Fluid Amplifier" McGraw-Hill, 1968.

2. _____, "Fluid Control Systems", Engineering Seminar on Fluid Control, Penn. State Univ., 1965.

3. Anderson, Blane W., "The Analysis and Design of Pneumatic System", John Wiley and Sons, Inc., 1967.

4. Oda, Migio, "Investigation of the Pulse Response of Fluid Logic Element", Second Fluidics Conference, Japan, August, 1968.

5. Willson, M.P., "The Switching Process in Bistable Fluid Amplifier", University of Connecticut, 1968.

6. Sawey, R.A., "Analysis of Time Dependent Jet Attachment Processes and Comparison with Experiment", Second Cranfield Fluidics Conference, 3rd-5th A2-17, January, 1967.

7. Brown, C.C., "Design and Manufacture of Pure Fluid Elements", Second Cranfield Fluids Conference 3rd-5th, F4-37, January, 1967.

8.   Bouteille, D., "New Approach and Recent Development
      in Piston Logic as Applied to General Automation",
      P3-46 Second Cranfield Fluidics Conference, 3rd-
      5th, January, 1967.

9.   Abbate-Daga, A., "Criteria for the Selection of Time
      Functions in the Design of Fluidic Automatisms",
      Third Cranfield Fluidics Conference, 8th-10th,
      K12-175, May, 1968.

10.   Bantle, K., Siemens, A.G., "Counters with Bistable
      Fluid Element", H5-73, Second Cranfield Fluidic
      Conference, January, 1967.

11.   Davis, G.E., "A Fluidic Method of Inlet Guide Vane
      Control for Jet Engines", IFAC, Volume 6, No. 4,
      July, 1970.

12.   Hicks, Tyler G., "Industrial Hydraulics", McGraw-
      Hill, Second Edition, 1970.

13.   Ward, E.J., Kemble, J.E., Wheeler, K.J., "A Lathe
      Control System in Corporating Fluidics", A4,
      Third Cranfield Fluidics Conference, May, 1968.

14.   Walters, R., "Hydraulic and Electro-Hydraulic Servo
      System", CRC Press, 1967.

15. Simson, A.K., "Gain Characteristic of Subsonic Pressure-
     Controlled, Proportional Fluid-Jet Amplifier",
     Basic Eng. pp 295, June, 1966.

16. Raven, Francis H., "Automatic Control Engineering",
     McGraw-Hill, Second Edition, 1968.

17. Gyorog, D.A., "The Notes of Fluid System and Control",
     April, 1970.

18. Gyorog, D.A., "Test of a Digital Fluidic Control Circuit"
     Boeing Company, August, 1967.

19. Belforte, G., "Low Frequency Oscillator", T-4, Third
     Cranfield Conference, May, 1968.

20. Lush, P.A., "Investigation of the Switching Mechanism
     in a Large Scale Model of a Turbulent Reattach-
     ment Amplifier", Second Cranfield Conference,
     January, 1967.

IX. VITA

Yu-Fang Yen was born on March 21, 1942 in Taiwan, China. He received his primary technical education from Taipei Institute of Technology in Taiwan. In 1967 he went to Japan for further study. He received a Bachelor of Engineering Degree in Mechanical Engineering from National Tohoku University in March, 1969.

He has been enrolled in the Graduate School of the University of Missouri-Rolla since September, 1969.